

CLUSTER ALGEBRAIC INTERPRETATION OF INFINITE FRIEZES

EMILY GUNAWAN, GREGG MUSIKER, AND HANNAH VOGEL

ABSTRACT. Originally studied by Conway and Coxeter, friezes appeared in various recreational mathematics publications in the 1970s. More recently, in 2015, Baur, Parsons, and Tschabold constructed periodic infinite friezes and related them to matching numbers in the once-punctured disk and annulus. In this paper, we study such infinite friezes with an eye towards cluster algebras of type D and affine A, respectively. By examining infinite friezes with Laurent polynomial entries, we discover new symmetries and formulas relating the entries of this frieze to one another. Lastly, we also present a correspondence between Broline, Crowe and Isaacs's classical matching tuples and combinatorial interpretations of elements of cluster algebras from surfaces.

CONTENTS

1. Introduction	2
Acknowledgments	4
2. Cluster algebras from surfaces	4
2.1. Triangulations of marked surfaces	4
2.2. From surfaces to cluster algebras	6
2.3. Generalized arcs and closed loops	6
2.4. Laurent polynomials associated to generalized arcs and closed loops	8
3. Infinite friezes	11
4. Infinite friezes of cluster algebra elements	15
5. Progression formulas	16
5.1. Complementary arcs	17
5.2. Proof of Theorem 5.4	18
6. Bracelets and growth coefficients	21
6.1. Growth coefficients	21
6.2. Chebyshev polynomials	22
7. Recursive relationships	23
7.1. Differences from complement symmetry	23
7.2. Arithmetic progressions	24
Appendix A. A bijection between BCI tuples and T-paths	26
A.1. BCI tuples and T -paths	26
A.2. Cluster expansion formula in terms of BCI tuples	28
A.3. Proof that the trail map sends BCI tuples to T -paths	29
A.4. Triangles map	32
A.5. Natural lattice structure of the BCI tuples	33
References	36

2010 *Mathematics Subject Classification.* 13F60 (primary), 05C70, 05E15 (secondary).

Key words and phrases. cluster algebra, Conway-Coxeter frieze, frieze pattern, infinite frieze, triangulation, marked surface.

1. INTRODUCTION

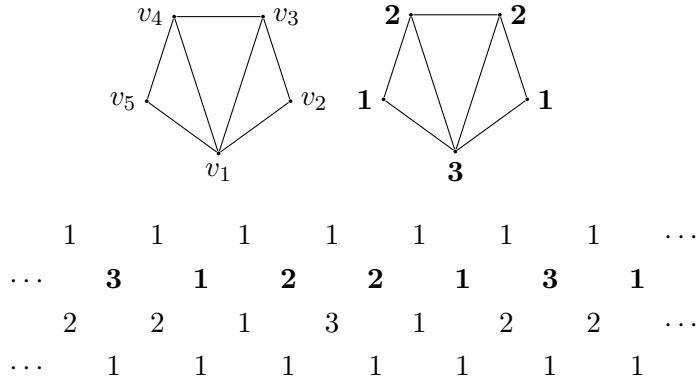
A *finite frieze* is an array of bi-infinite (infinite along the positive and negative x -axis) rows of positive integers, bounded above and below by a row of 1s, such that, for every diamond

$$\begin{array}{ccc} & c & \\ a & & b \\ & d & \end{array}$$

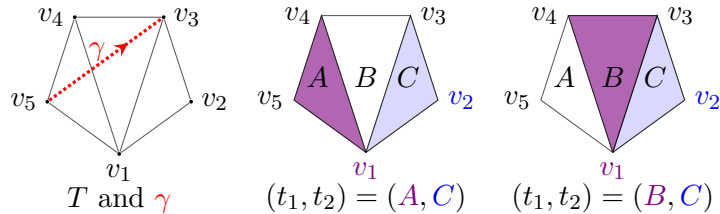
of entries in the frieze, the equation $ab - cd = 1$ is satisfied. We say that a frieze has period n if the rows repeat after n entries. Note that n may not be minimal.

If every entry in the frieze is a positive integer, then it is said to be a *frieze of positive integers*. Finite friezes of positive integers were first studied by Coxeter [Cox71], and then by Conway and Coxeter [CC73]. They showed that these patterns are invariant under a glide reflection, and give a bijection between finite friezes and triangulations of polygons.

The first non-trivial row (*i.e.*, the row following the row of 1s) of a frieze consists of infinitely many repeated copies of a *quiddity sequence*. The quiddity sequence defines a finite frieze, and the entries of this sequence can be read off directly from a corresponding triangulation. The period n is the number of marked points on the boundary of the associated triangulated polygon. We label vertices v_1, \dots, v_n counter-clockwise around a triangulated polygon (we often write i for vertex v_i), and for each vertex v_i , the corresponding entry a_i in the quiddity sequence (a_1, \dots, a_n) is the number of triangles incident to i in T . See the following for an example.



In [BCI74], Broline, Crowe, and Isaacs further studied the geometry of these finite frieze patterns associated to triangulations of polygons. Given a triangulation T , they found that every entry in such a frieze corresponds to a *matching number* associated to a diagonal. In particular, to any such diagonal, they associate a set of vertices v_{i_1}, \dots, v_{i_r} (those lying to the right) and then match these to an r -tuple (t_1, \dots, t_r) of pairwise-distinct triangles in T , such that t_j is incident to vertex v_{i_j} . We refer to this r -tuple as a *BCI tuple*. For example, the diagonal from v_5 to v_3 is associated to the vertices v_1 and v_2 . There are exactly two BCI 2-tuples corresponding to v_1 and v_2 , as we illustrate below.



Caldero and Chapoton in [CC06] showed that finite frieze patterns appear in the context of cluster algebras of type A . Baur and Marsh in [BM09] used matching numbers to consider finite frieze patterns coming from triangulations of once-punctured disks, and thereby gave a definition

of a finite frieze pattern corresponding to a cluster algebra of type D . See also [Sch08b] by Schiffler, for his study of the corresponding cluster category.

A frieze is said to be *infinite* if it is not bounded below by a row of 1's. Infinite friezes (of positive integers) arising from triangulations of once-punctured disks were introduced and studied in [Tsc15] by Tschabold. Given an ideal triangulation T (in the sense of [FST08]) of a once-punctured disk with n marked boundary points labeled $1, 2, \dots, n$ counterclockwise around the boundary (note: this is the opposite to the convention in [Tsc15]), we can read off a quiddity sequence for the corresponding frieze pattern in a similar way. See Fig. 1.

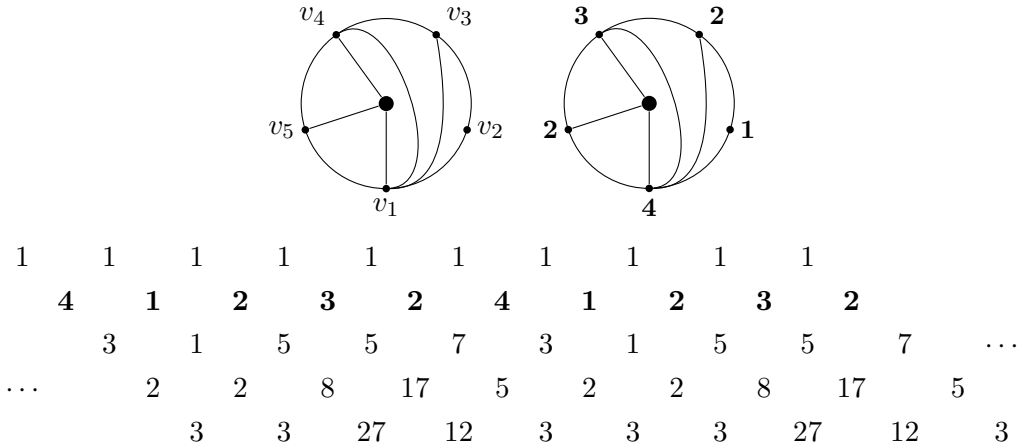


FIGURE 1. First *level* (see Section 6.1) of an infinite frieze pattern corresponding to a once-punctured disk.

A finite frieze pattern that is associated to a triangulation of a polygon is said to be of type A . In [BPT16], Baur, Parsons, and Tschabold provide a complete classification of infinite frieze patterns. An infinite frieze pattern is said to be of type D or type \tilde{A} , if is associated to a triangulation of a once-punctured disk or annulus, respectively. Other work on frieze patterns of type D and \tilde{A} include [Smi15, BFPT16].

In this paper, we study infinite friezes whose entries are Laurent polynomials (as opposed to positive integers). Our first result (Theorem 4.1) is a construction of an infinite frieze where the entries of the frieze correspond to Laurent polynomials associated to generalized peripheral arcs. We go on to describe nice symmetries and properties that this frieze pattern satisfies. In Section 5, we introduce *complementary arcs*, which are arcs between the same two vertices in a surface, but of alternate direction. Complementary arcs give rise to a special type of symmetry, which we call *complement symmetry*, in an infinite frieze. This complement symmetry reduces to glide-symmetry in a finite frieze pattern because complementary arcs in a polygon give rise to the same entry (matching number/arc/Laurent polynomial) in a finite frieze. We use these complementary arcs to describe *progressions* of arcs in the frieze (Theorem 5.4). In Section 6, we discuss *growth coefficients* (first defined in [BFPT16]) of the frieze, and show that they are equal to Laurent polynomials corresponding to certain curves called *bracelets* in the surface. Bracelets are associated to important cluster algebra elements which have been studied by many, including [SZ04, DT13, MW13, MSW13, Thu14, CS15a, CS15b]. In Section 7, we state further algebraic and combinatorial results involving the relationship between complementary arcs. Finally, in Appendix A, we extend previous unpublished work of Carroll-Price [CP03] to provide a bijection

between BCI tuples [BCI74] and T -paths (as in [Sch08a, ST09]). Our bijection yields an expansion formula for cluster variables in terms of BCI tuples (Corollary A.8) and preserves a natural distributive lattice structure which the T -paths are known to have (Proposition A.19).

We begin our article with Section 2, which introduces the necessary background material, including the notation and terminology of arcs, triangulations, and cluster algebras that we will use throughout the article. We also recall cluster algebra elements associated to generalized arcs and closed loops (with or without self-crossings) via snake graphs and band graphs, as per [MW13, MSW11, MSW13]. Then in Section 3, we recall some facts about infinite friezes, and explain how triangulations (of once-punctured disks and annuli) give rise to infinite friezes. The remainder of our article provides the statements of our results and their proofs as previewed above.

ACKNOWLEDGMENTS

E. Gunawan and G. Musiker were supported by NSF Grants DMS-1148634 and DMS-1362980. H. Vogel was supported by the Austrian Science Fund (FWF): projects No. P25141-N26 and W1230, and acknowledges support from NAWI Graz. She would also like to thank the University of Minnesota for hosting her during her stay in the Winter of 2016.

We thank Karin Baur for helpful comments, and Manuela Tschabold for allowing us to use some of her tikz figures. Some of the images and Laurent polynomial computation was done with the help of SAGEMATH [Dev16, SCc08] and code written by Ana García Elsener and Jorge Nicolás López of Universidad Nacional de Mar del Plata.

2. CLUSTER ALGEBRAS FROM SURFACES

We provide a brief background on cluster algebras arising from marked surfaces following Fomin, Shapiro, and Thurston [FST08].

2.1. Triangulations of marked surfaces.

Definition 2.1 (marked surface). *Let S be a connected, oriented, Riemann surface with (possibly empty) boundary, and M a non-empty, finite set of marked points in the closure of S , such that there is at least one marked point on each boundary component of S . Then (S, M) is called a marked surface, and the interior points of S are called punctures.*

For technical reasons, assume that (S, M) is not the following: a sphere with fewer than four punctures; a monogon with zero or one puncture; or a bigon or triangle without punctures.

Definition 2.2 (ordinary arc). *An ordinary arc γ in (S, M) is a curve in S , considered up to isotopy, such that: (1) the endpoints of γ are in M , (2) γ does not cross itself (except its endpoints may coincide), (3) the interior of γ is disjoint from M and from the boundary of S , and (4) γ does not cut out an unpunctured monogon or bigon. A boundary edge is a curve that connects two marked points and lies entirely on the boundary of S without passing through a third marked point.*

We say that two ordinary arcs α, β are *compatible* if there exist representatives α', β' in their respective isotopy classes such that α' and β' do not intersect in the interior of S .

Definition 2.3 (ideal triangulation). *An ideal triangulation is a maximal (by inclusion) collection of distinct, pairwise compatible ordinary arcs. The ordinary arcs of an ideal triangulation cut the surface into ideal triangles (see Fig. 2).*

Remark 2.4 (possible types of ideal triangles). *There are two types of ideal triangles in a triangulation: triangles that have three distinct sides (Figs. 2(a), 2(b), and 2(c)), and self-folded triangles (Fig. 2(d)). A self-folded triangle consists of an arc ℓ (which we will refer to as an ℓ -loop) whose endpoints coincide, along with an arc r (called a radius) that goes from the endpoint of ℓ to an enclosed puncture.*

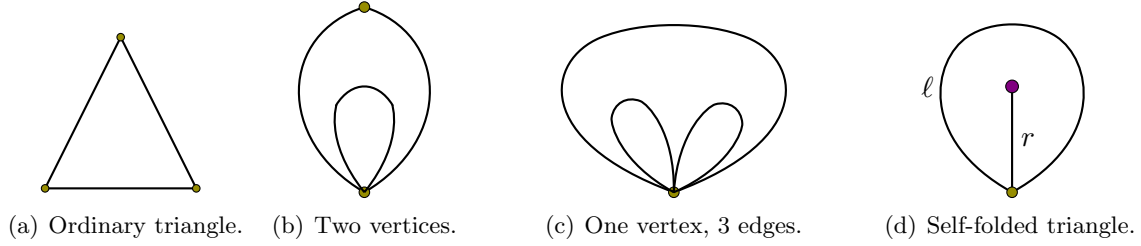


FIGURE 2. Possible types of ideal triangles.

Definition 2.5 (peripheral and radial arcs). *Let γ be an ordinary arc of a surface (S, M) with nonempty boundary. Following [DT13, BD14], we say that γ is a peripheral arc if: (1) both its endpoints (or its unique endpoint in the case of a loop) are on a single boundary component Bd of S , and (2) γ is isotopic to a concatenation of two or more boundary edges of a boundary component Bd . We call an arc connecting a marked point on a boundary component to a puncture (or a different boundary component) a radial arc.*

Definition 2.6 (flip for ordinary arc). *A flip is a move that replaces an ordinary arc γ in an ideal triangulation T with a unique arc $\gamma' \neq \gamma$ such that $(T \setminus \gamma) \cup \gamma'$ forms a new ideal triangulation.*

Any two ideal triangulations of a surface are connected to each other by a sequence of flips (see Fig. 3 for an example).

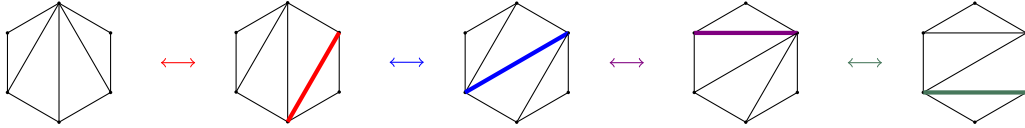


FIGURE 3. Sequence of flips.

When working with a cluster algebra associated to a surface with punctures, it is not sufficient to work with ordinary arcs and ideal triangulations. The authors of [FST08] introduced *tagged arcs* and *tagged triangulations*, and showed that they are in bijection with cluster variables and clusters.

Definition 2.7 (tagged arcs). *A tagged arc is obtained by taking an ordinary arc (that is not an ℓ -loop) γ and marking (“tagging”) each end γ with one of two options, plain or notched, such that:*

- 1) *an endpoint lying on the boundary must be tagged plain, and*
- 2) *both ends of a loop must be tagged the same way.*

A notched tagging is usually indicated by a bow tie, and a plain tagging is usually denoted by no marking. Note that a tagged arc never cuts out a once-punctured monogon, i.e., an ℓ -loop is not a tagged arc. For a list of tagged arcs, see [FST08, Remark 7.3].

Compatibility of two tagged arcs is defined in [FST08, Def. 7.4]. A maximal (by inclusion) collection of distinct, pairwise compatible tagged arcs is called a *tagged triangulation*. Fig. 4 (center) gives an example of a tagged triangulation. The *flip* of a tagged arc is defined in [FST08, Section 9.3].

Definition 2.8 (representing ordinary arcs as tagged arcs). *Any ordinary arc γ can be represented by a tagged arc $\iota(\gamma)$ as follows. Suppose γ is an ℓ -loop (based at marked point v) which encloses a puncture p . Let r be the unique arc which is compatible with γ and which connects v and p . Then $\iota(\gamma)$ is obtained by tagging r plain at v and notched at p . Otherwise, $\iota(\gamma)$ is simply γ tagged plain at both endpoints. For example, see Fig. 4(left & center).*

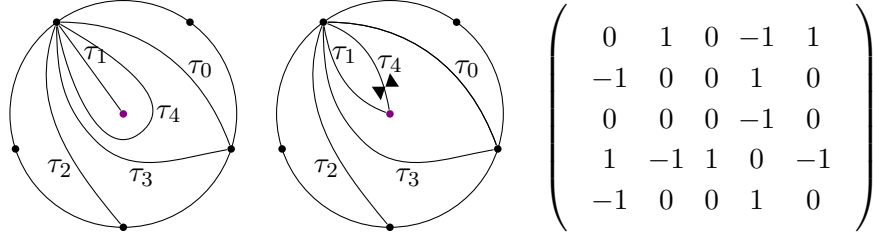


FIGURE 4. An ideal triangulation & a corresponding tagged triangulation of the once-punctured 5-gon, and the corresponding signed adjacency matrix.

2.2. From surfaces to cluster algebras. We can associate an exchange matrix [FST08, Def. 4.1 and 9.6], and hence a cluster algebra, to (S, M) . Note that our convention agrees with [Sch10, MS10] but is opposite of the more recent papers [MSW11, MW13, MSW13].

Definition 2.9 (signed adjacency matrix of an ideal triangulation). *Let T be an ideal triangulation, and $\tau_1, \tau_2, \dots, \tau_n$ arcs of T . For any non-self folded triangle Δ in T , we define a matrix $B^\Delta = (b_{ij}^\Delta)_{1 \leq i \leq n, 1 \leq j \leq n}$ as follows:*

- $b_{ij}^\Delta = 1$ and $b_{ji}^\Delta = -1$ in the following cases:
 - (a) τ_i and τ_j are sides of Δ with τ_j following τ_i in the counterclockwise order;
 - (b) τ_j is a radial arc in a self-folded triangle enclosed by an ℓ -loop τ_ℓ , and τ_i and τ_ℓ are sides of Δ with τ_ℓ following τ_i in the counterclockwise order;
 - (c) τ_i is a radial arc in a self-folded triangle enclosed by an ℓ -loop τ_ℓ , and τ_ℓ and τ_j are sides of Δ with τ_j following τ_ℓ in the counterclockwise order;
- $b_{ij}^\Delta = 0$ otherwise.

Then define the signed adjacency matrix $B_T = (b_{ij})_{1 \leq i \leq n, 1 \leq j \leq n}$ of T by $b_{ij} = \sum_{\Delta} b_{ij}^\Delta$, where the sum is taken over all triangles in T that are not self-folded.

Definition 2.10 (signed adjacency matrix of a tagged triangulation). *Let T be a tagged triangulation. From T , we construct a tagged triangulation \hat{T} as follows: for each puncture such that all endpoints are notched, we change their tags to plain. Let T° be the ideal triangulation which is represented by \hat{T} . For each tagged arc in T , the corresponding ordinary arc in T° retains the same label. The signed adjacency matrix B_T of T is defined to be the signed adjacency matrix B_{T° of T° (as in Definition 2.9). See Fig. 4(right) for an example.*

Theorem 2.11 ([FST08] Theorem 7.11, and [FT12] Theorem 6.1). *Let (S, M) be a marked surface, and let $\mathcal{A} = \mathcal{A}(S, M)$ be the coefficient-free cluster algebra associated to the signed adjacency matrix of a tagged triangulation (as in Definition 2.10). Then the (unlabeled) seeds Σ_T of \mathcal{A} are in bijection with tagged triangulations T of (S, M) , and the cluster variables are in bijection with the tagged arcs of (S, M) (so we can denote each cluster variable by x_γ or $x(\gamma)$, where γ is a tagged arc). Moreover, each seed in \mathcal{A} is uniquely determined by its cluster. Furthermore, if a tagged triangulation T' is obtained from another tagged triangulation T by flipping a tagged arc $\gamma \in T$ and obtaining γ' , then $\Sigma_{T'}$ is obtained from Σ_T by the seed mutation replacing x_γ by $x_{\gamma'}$.*

If ℓ is an unnotched ℓ -loop which encloses a radius r and a puncture P , then we set $x_\ell = x_r x_{r(P)}$, where $r^{(P)}$ denote the arc obtained from r by changing its notching at P . If τ is a boundary edge, we set $x_\tau := 1$.

2.3. Generalized arcs and closed loops. In [MSW11], the second author, Schiffler, and Williams gave a combinatorial formula for the Laurent expansion of any cluster variable in a cluster algebra associated to a marked surface. Their expansion formula, which is a weighted sum over perfect

matchings of a *planar snake graph*, associates a cluster algebra element to an arc in the surface. In [MSW13, MW13], the same authors generalized this construction and associated cluster algebra elements to *generalized arcs*, as well as to *closed loops* (with or without self-crossings). Instead of perfect matchings of a planar graph, the Laurent polynomial associated to a closed curve is a weighted sum over good matchings in a *band graph* on a Mobius strip or annulus. In coefficient-free settings, these constructions for generalized arcs and loops work even in the existence of punctures.

Definition 2.12 (generalized arcs). *A generalized (ordinary) arc in (S, M) is a curve γ in S , considered up to isotopy, such that*

- (1) *the endpoints of γ are in M ,*
- (2) *the interior of γ is disjoint from M and the boundary of S , and*
- (3) *γ does not cut out an unpunctured bigon or monogon. In other words, γ is not contractible to a point, and γ is not isotopic to a boundary edge.*

Generalized arcs are allowed to intersect themselves a finite number of times (possibly 0). We consider these arcs up to isotopy of immersed arcs, that is, allowing Reidemeister moves of types II and III but not of type I. In particular, an isotopy cannot remove a contractible kink from a generalized arc. If an arc intersects itself, we say that the arc has a self-crossing.

Definition 2.13 (generalized peripheral arc). *Suppose (S, M) contains a boundary component Bd . We say that a generalized (ordinary) arc γ is a generalized peripheral arc on Bd if γ starts at a marked point on Bd , wraps finitely (possibly 0) many times around Bd and then ends at a marked point on Bd (possibly at the same starting point). Furthermore, as in Definition 2.5, a generalized peripheral arc on Bd is isotopic to a concatenation of two or more boundary edges of Bd . Our convention is to choose the orientation of γ so that Bd is to the right of γ when looking from above.*

Remark 2.14. *In the case of the once-punctured disk (respectively, annulus), we can draw a generalized arc in the universal cover as in [BPT16, Sec. 3.3]. In the universal cover, we identify generalized peripheral arcs $\gamma(i, j)$ on the (lower) boundary with their two endpoints, labeled with $i, j \in \mathbb{Z}$.*

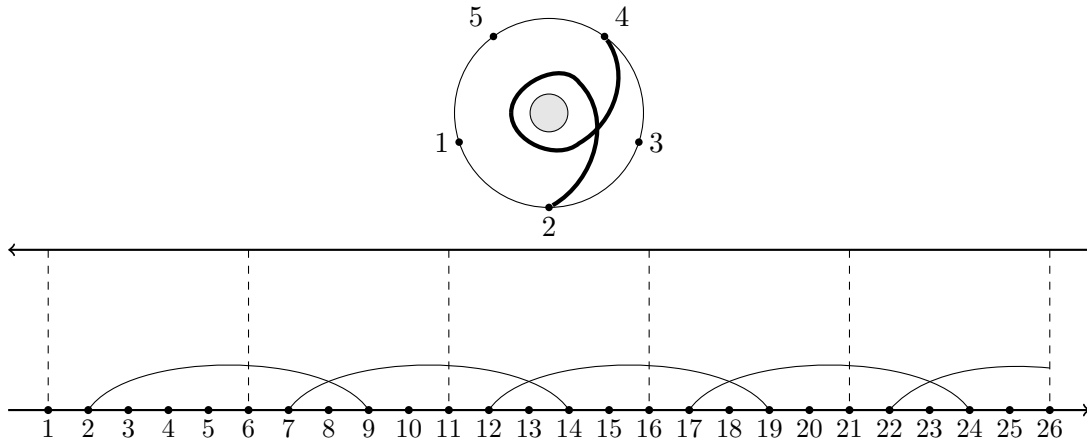


FIGURE 5. Top: The generalized peripheral arc $\gamma(2, 9)$. Bottom: Universal cover of the annulus $C_{n,m}$, for $n = 5$.

Example 2.15. *In Fig. 5, we draw copies of the arc $\gamma(2, 9)$ (top figure) along the lower (outer) boundary in the universal cover of an annulus with 5 points on the outer boundary (bottom figure). Note that the arc $\gamma(2, 9)$ has a self-crossing in the annulus. This can be seen in the universal cover by the arc crossing into another frame (denoted by the dashed lines).*

Definition 2.16 (closed loops). *A closed loop in (S, M) is a closed curve γ in S which is disjoint from the boundary of S . Again, we allow closed loops to have a finite number of self-crossings, and we consider closed loops up to isotopy.*

Definition 2.17 (bracelets). *A closed loop obtained by following a (non-contractible, non-self-crossing, kink-free) loop k times, and thus creating $k - 1$ self-crossings, is called a k -bracelet and is denoted by $Brac_k$. See Fig. 6.*

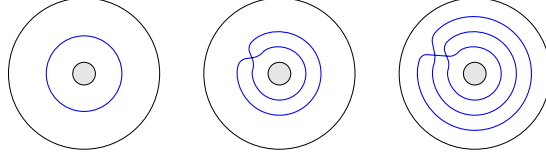


FIGURE 6. Bracelets $Brac_1$, $Brac_2$, and $Brac_3$.

2.4. Laurent polynomials associated to generalized arcs and closed loops. Recall from Theorem 2.11 that for unlabeled seeds Σ_T of a cluster algebra \mathcal{A} , the tagged arcs of (S, M) are in bijection with the cluster variables, and we denote these variables by x_τ for τ a tagged arc.

Definition 2.18 (snake graph). *A snake graph is a connected sequence of square tiles embedded in the plane. To build a snake graph, start with one tile, then glue a new tile so that the new tile is glued to the north or the east of the previous tile. Let γ be an ordinary generalized arc which is not an arc of an ideal triangulation T . A snake graph associated to γ and T is a weighted graph which is defined in [MSW11, MW13] (see also [CS13]). For example, see Fig. 8.*

Definition 2.19 (band graph). *A band graph, which lies on an annulus or a Möbius strip, is obtained from identifying two edges of a snake graph. Let ζ be a loop. A band graph associated to ζ and an ideal triangulation T is as defined in [MW13, MSW13] (see also [CS15a]). For example, see Fig. 10.*

Definition 2.20 (crossing monomial). *If γ is a generalized arc of a closed loop, and $\tau_{i_1}, \tau_{i_2}, \dots, \tau_{i_d}$ is the sequence of arcs in T which γ crosses, then the crossing monomial of γ with respect to T is defined to be (see, for example, [MSW11, Def. 4.5])*

$$\text{cross}(T, \gamma) = \prod_{j=1}^d x_{\tau_{i_j}}.$$

Recall that if τ is a boundary segment, we let $x_\tau := 1$.

Definition 2.21 (weight of a perfect matching). *A perfect matching of a graph G is a subset P of the edges of G such that each vertex of G is incident to exactly one edge of P . If G is a snake or band graph, and the edges of a perfect matching P of G are labeled $\tau_{j_1}, \dots, \tau_{j_r}$, then we define the weight $x(P)$ of P to be $x_{\tau_{j_1}} \cdots x_{\tau_{j_r}}$. See [MW13, Def. 3.7].*

Definition 2.22 (Laurent polynomial from a generalized arc). *Let (S, M) be a surface, T an ideal triangulation, and \mathcal{A} the cluster algebra associated to B_T . Let γ be a generalized arc and let $G_{T, \gamma}$ denote its snake graph. We define a Laurent polynomial which lies in (the fraction field) of \mathcal{A} .*

- (1) *If γ cuts out a contractible monogon, then X_γ^T is equal to zero.*
- (2) *If γ has a contractible kink, let $\bar{\gamma}$ denote the corresponding tagged arc with this kink removed, and define $X_\gamma^T := (-1)X_{\bar{\gamma}}^T$.*

(3) Otherwise, define

$$X_\gamma^T := \frac{1}{\text{cross}(T, \gamma)} \sum_P x(P),$$

where the sum is over all perfect matchings P of $G_{T, \gamma}$.

See [MW13, Def. 3.12].

Theorem 2.23 ([MSW11, Thm 4.10]). *When γ is an arc (with no self-crossings), X_γ^T is equal to the Laurent expansion of the cluster variable $x_\gamma \in \mathcal{A}$ with respect to the seed Σ_T .*

Definition 2.24 (good matching of a band graph). *Let ζ be a closed loop. A perfect matching P of the band graph $\tilde{G}_{T, \zeta}$ is called a good matching if there exists at least one tile of $\tilde{G}_{T, \zeta}$ with two of its four edges as part of P . For a precise definition, see [MW13, Def. 3.18].*

We can now define a Laurent polynomial X_ζ for every closed loop ζ .

Definition 2.25 (Laurent polynomial from a closed loop). *Let (S, M) be a surface, T an ideal triangulation, and \mathcal{A} the cluster algebra associated to B_T . Let ζ be a closed loop. We define a Laurent polynomial X_ζ^T which lies in (the fraction field) of \mathcal{A} .*

- (1) If ζ is a contractible loop, then let $X_\zeta^T := -2$.
- (2) If ζ is a closed loop without self-crossings enclosing a single puncture p , then $X_\zeta^T := 2$.
- (3) If ζ has a contractible kink, let $\bar{\zeta}$ denote the corresponding closed loop with this kink removed, and define $X_\zeta^T := (-1)X_{\bar{\zeta}}$.
- (4) Otherwise, let

$$X_\zeta^T := \frac{1}{\text{cross}(T, \gamma)} \sum_P x(P),$$

where the sum is over all good matchings P of the band graph $\tilde{G}_{T, \zeta}$.

See [MW13, Def. 3.21].

In our study of infinite friezes, we only consider marked surfaces (S, M) which have nonempty boundary. In this situation, the Laurent polynomials given in Definitions 2.22 and 2.25 in fact lie in \mathcal{A} , due to [MSW13, Proposition 4.5], [Mul13, Theorem 4.1] and [CLS15, Theorem 5].

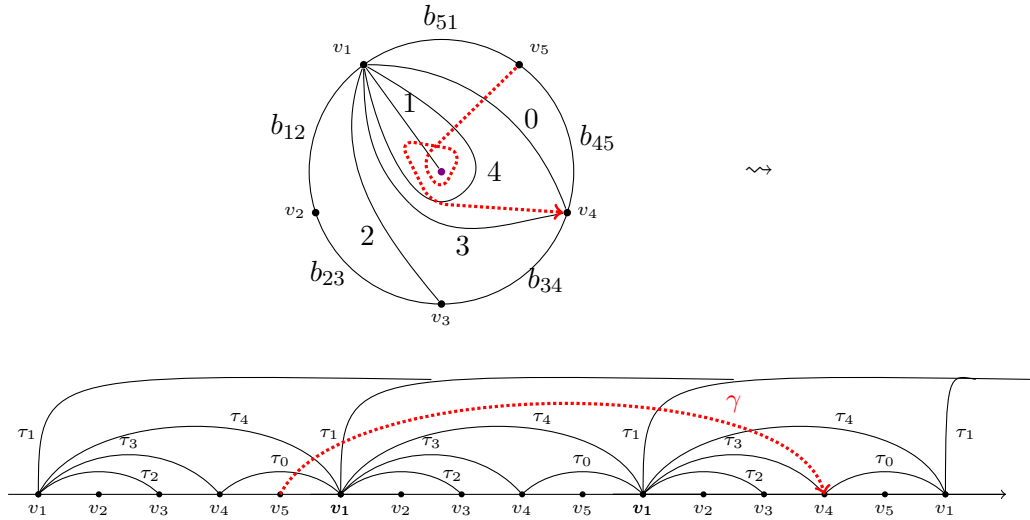


FIGURE 7. Top: An ideal triangulation T and a generalized arc γ of a once-punctured disk. Bottom: T drawn on a strip.

		1	1	4	0			
0	4	1	1	4	1	1	4	3
b_{45}	3		4		1		1	
	0		4					
								b_{51}

FIGURE 8. The snake graph corresponding to the generalized arc γ of Fig. 7.

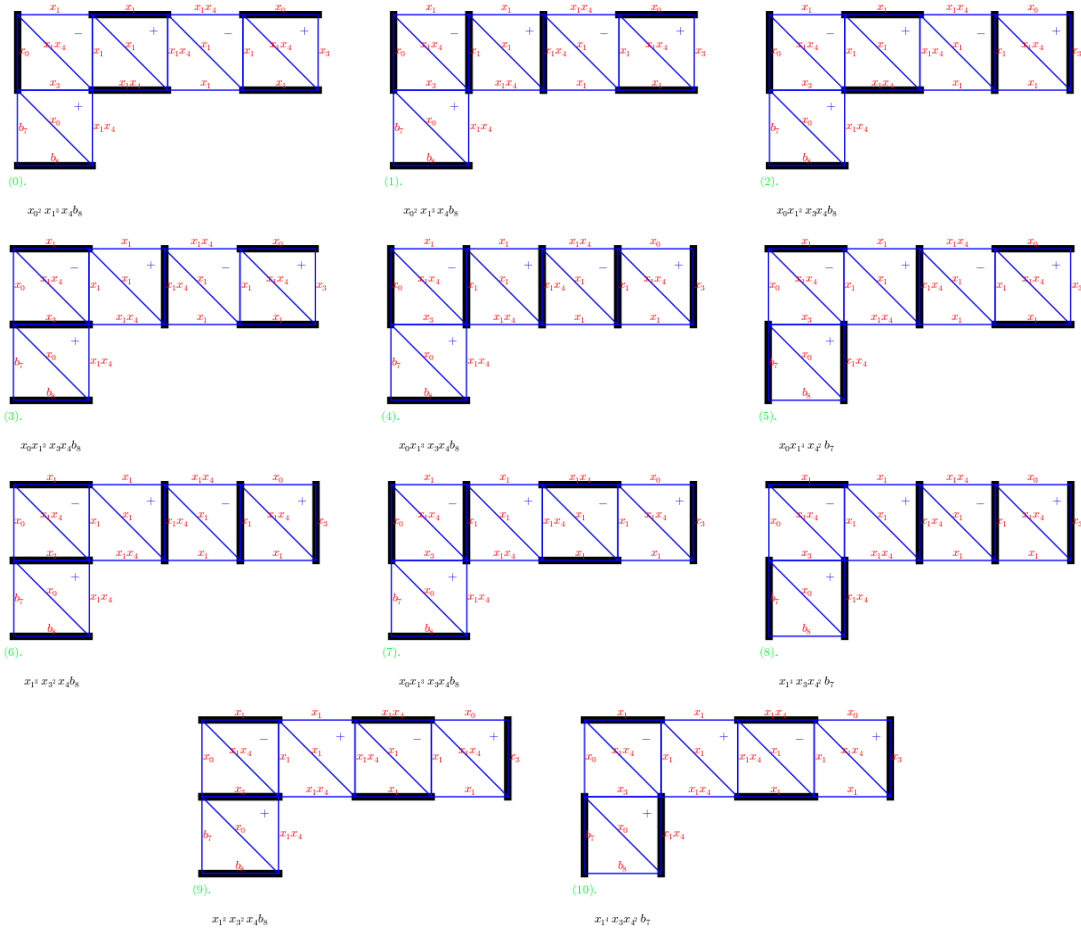


FIGURE 9. The 11 perfect matchings of the snake graph from Fig. 8, created using the help of SAGEMATH [Dev16, SCC08].

Example 2.26 (example of a Laurent expansion corresponding to a generalized arc). *Consider the ideal triangulation T of a once-punctured disk and a generalized arc in Fig. 7. We obtain the snake graph $G_{T,\gamma}$ in Fig. 8. Following Definition 2.22, we compute*

$$X_\gamma^T = \frac{x_0 x_1 x_4 + 2x_1 x_3 x_4 + 2x_0^2 + 4x_0 x_3 + 2x_3^2}{x_0 x_1 x_4}$$

by specializing $x(\tau) = 1$ for each boundary edge τ . In particular, the snake graph $G_{T,\gamma}$ has 11 perfect matchings (see Fig. 9).

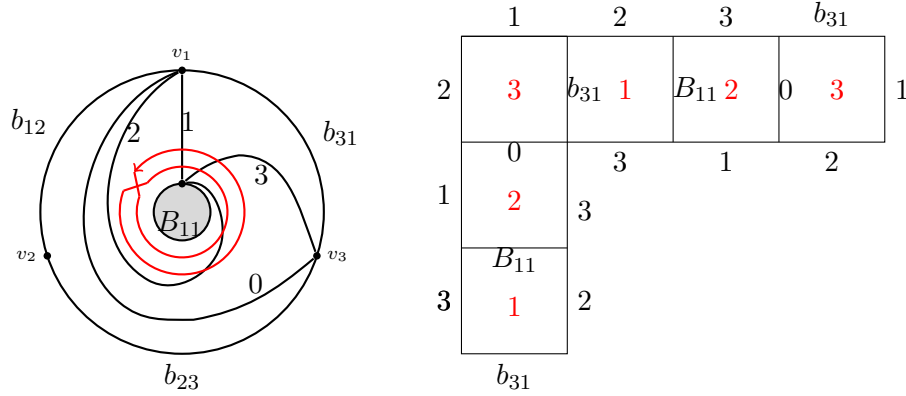


FIGURE 10. Left: An ideal triangulation T and the bracelet $Brac_2$. Right: Corresponding band graph $\tilde{G}_{T,\gamma}$.

Example 2.27 (Example of the Laurent polynomial corresponding to $Brac_2$ in an annulus). Consider the ideal triangulation T of an annulus and the $Brac_2$ in Fig. 10 (left). We obtain the graph $\tilde{G}_{T,Brac_2}$ in Fig. 10 (right). Following Definition 2.25, we compute

$$X_{Brac_2}^T = \frac{x_1^4 x_3^2 + x_2^4 x_3^2 + 2x_0 x_1^3 x_3 + 2x_0 x_1 x_2^2 x_3 + x_0^2 x_1^2 + 2x_1^2 x_2 x_3 + 2x_2^3 x_3 + 2x_0 x_1 x_2 + x_2^2}{x_1^2 x_2^2 x_3^2}$$

by specializing $x(\tau) = 1$ for each boundary edge τ . In particular, the band graph $\tilde{G}_{T,Brac_2}$ has 14 good matchings (see Fig. 11).

For the rest of the paper, we will use the notation x_γ or $x(\gamma)$ to denote the cluster algebra element corresponding to γ , where γ is a generalized arc or loop.

3. INFINITE FRIEZES

Tschabold in [Tsc15] showed that triangulations of once-punctured disks give rise to certain periodic (positive integral) infinite friezes, and that infinite friezes arising in this way satisfy a certain arithmetic property (see Section 7.2). In [BPT16], Baur, Parsons, and Tschabold went further and gave a complete characterization of infinite frieze patterns of positive integers via triangulations of quotients of an infinite strip in the plane. In this classification, periodic frieze patterns arise from triangulations of the annulus (which can be thought of as a quotient of the infinite strip by translation) or of the once-punctured disk. We refer the reader to Lemma 3.6 of [BPT16] for a description on how to draw a triangulation of a once-punctured disk as an asymptotic triangulation in the infinite strip. See an example in Fig. 12.

Definition 3.1. An infinite frieze \mathcal{F} of positive integers is an array $\{m_{ij}\}_{i,j \in \mathbb{Z}, j \geq i}$ with infinitely many rows, drawn as in Fig. 13, such that $m_{i,i} = 0$, $m_{i,i+1} = 1$, $m_{ij} \in \mathbb{Z}_{>0}$ for all $i \leq j$, where, for every diamond in \mathcal{F} indexed by

$$\begin{array}{ccc} & (i+1, j) & \\ (i, j) & & (i+1, j+1) \\ & (i, j+1) & \end{array}$$

the relation $m_{i,j} m_{i+1,j+1} - m_{i+1,j} m_{i,j+1} = 1$ is satisfied. We say that the row of all 0s is the zeroth row.

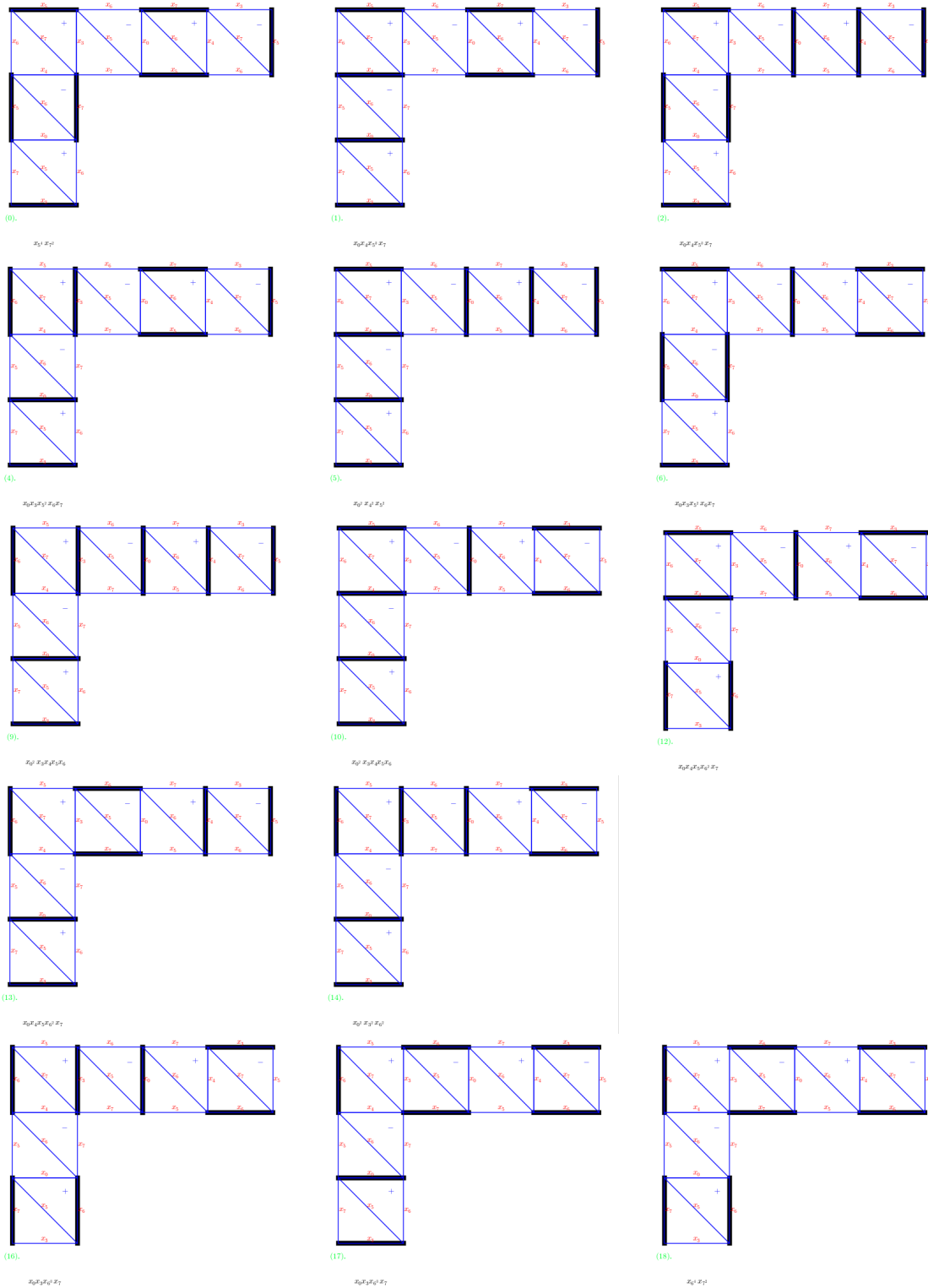


FIGURE 11. The 14 good matchings of the band graph from Fig. 10, created using the help of SAGEMATH [Dev16, SCc08].

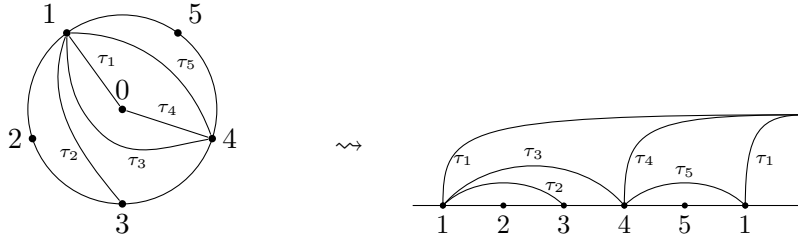


FIGURE 12. Triangulation of D_5 drawn as an asymptotic triangulation (see [BD14, Definition 3.3]).

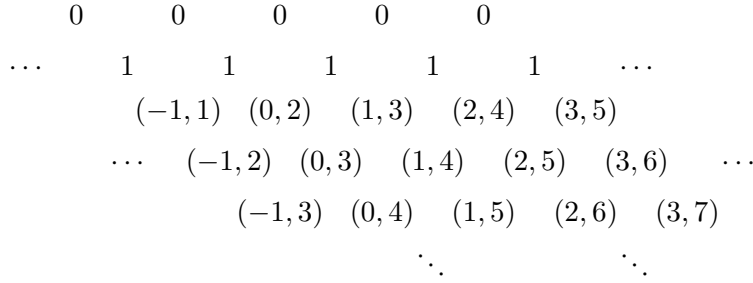


FIGURE 13. Indexing for an infinite frieze \mathcal{F} .

We often omit the row of 0s when writing a frieze pattern, as they do not provide any additional information. The first non-trivial row of a frieze (that is, the second row) is called a *quiddity row*. If \mathcal{F} is periodic with period n , then we call the n -tuple (a_1, \dots, a_n) a *quiddity sequence*.

Just as finite friezes of type A_n correspond to triangulations of a polygon P_{n+3} , triangulations of the once-punctured disk D_n give rise to infinite friezes of positive integers via matching numbers. Given a triangulation T of a once-punctured disk D_n , let the *quiddity sequence of T* be $q_T = (a_1, \dots, a_n)$ where a_i is the number of ideal triangles incident to a vertex i , such that, if i is adjacent to a self-folded triangle, both the self-folded triangle and the triangle with an ℓ -loop as one of its three sides, are counted twice. See Fig. 14 for an example of computing these matching numbers.

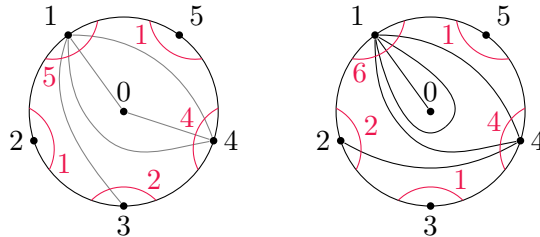


FIGURE 14. Counting triangles adjacent to boundary points in a triangulation of a once-punctured disk. Left: Triangulation without a self-folded triangle. Right: Triangulation with a self-folded triangle. Note that each of the two triangles with an ℓ -loop as a side is counted twice for vertex 1.

Now that we have a way to read off the quiddity sequence from a triangulation, we can construct an infinite frieze pattern. The frieze pattern coming from the quiddity sequence of Fig. 14 (left) is given in Fig. 15. We write the (kn) -th rows (for $k \in \mathbb{N}$) of the frieze in bold characters.

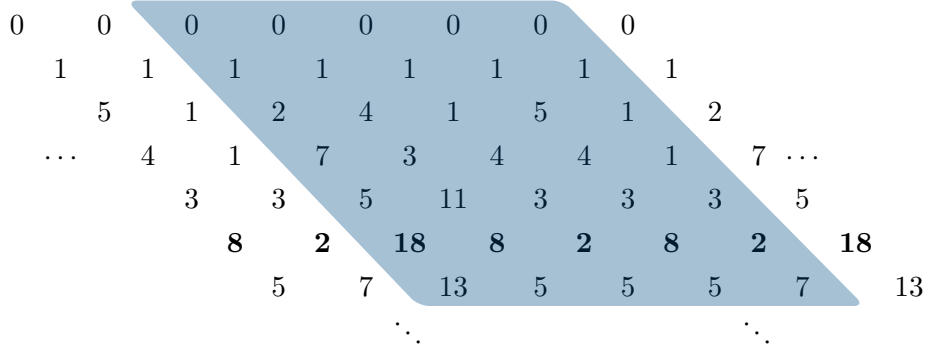


FIGURE 15. Infinite frieze with quiddity sequence $(2, 4, 1, 5, 1)$, with shaded fundamental region.

Theorem 3.2 ([Tsc15, Thm 3.6]). *Let T be a triangulation of a once-punctured disk D_n . Then the quiddity sequence $q_T = (a_1, \dots, a_n)$ of T is a quiddity sequence of an infinite frieze \mathcal{F}_T of period n .*

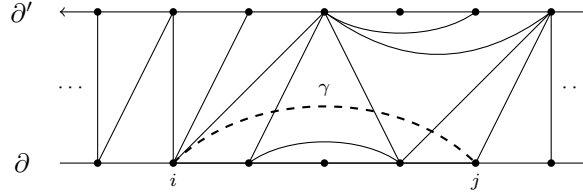
Remark 3.3. *In [BM09], Baur and Marsh provide a construction of finite periodic frieze patterns from once-punctured disks. The entries of their friezes are in bijection with indecomposables of a type D_n quiver and have the same form as the associated Auslander-Reiten quiver (e.g. see [Sch08b]). The friezes of Baur-Marsh match up with the first level (see Section 6.1) of the infinite friezes studied in this paper except that the two rows of theirs associated to the leaves of the fork in the D_n Dynkin diagram must be multiplied together point-wise to obtain the n th row in the infinite frieze.*

Consider a triangulation of the annulus $C_{n,m}$, where the outer boundary component has n marked points, and the inner boundary component has m marked points. Each of the outer boundary and inner boundary gives a quiddity sequence, and thus an infinite frieze. Unless otherwise stated, we consider the quiddity sequence coming from the outer boundary of an annulus.

Definition 3.4 ([BPT16, Def. 3.8]). *Let (a_1, \dots, a_n) be the quiddity sequence of a periodic frieze. We say that (a_1, \dots, a_n) can be realized in an annulus (resp. a once-punctured disk) if there is some $m \geq 1$ and a triangulation T of $C_{n,m}$ (resp. a triangulation T of D_n) such that (a_1, \dots, a_n) is the quiddity sequence of T .*

Let \mathcal{U} be the universal cover as described in Section 3.3 of [BPT16]. Then every quiddity sequence can be realized in \mathcal{U} , and every triangulation of \mathcal{U} gives rise to an infinite frieze (Theorem 5.2, [BPT16]). Every entry of these infinite friezes can still be described in terms of matching numbers. We can even consider non-periodic infinite friezes, which can be obtained via non-periodic triangulations of an infinite strip (without any quotienting).

Example 3.5. *Let T be the following triangulation of \mathcal{U} , and $\gamma(i, j)$ be the arc from i to j on the outer boundary ∂ :*



Then the arc $\gamma(i, j)$, corresponds to the (i, j) -th entry in the infinite frieze pattern arising from this triangulation.

4. INFINITE FRIEZES OF CLUSTER ALGEBRA ELEMENTS

Our first result is the construction of infinite frieze patterns consisting of certain elements of a cluster algebra.

Theorem 4.1. *Let T be an ideal triangulation of a once-punctured disk or an annulus, and let $\mathcal{A} = \mathcal{A}(B_T)$ be the coefficient-free cluster algebra associated to the signed adjacency matrix B_T . Let Bd be a boundary component with n marked points, where $n \geq 2$. Then the Laurent polynomials corresponding to generalized peripheral arcs on Bd form an infinite frieze pattern.*

Before we prove the theorem, we recall *skein relations*, and the related terminology.

Definition 4.2. *A multicurve is a finite multiset of generalized arcs and closed loops such that there are only a finite number of pairwise crossings among the collection. A multicurve is said to be simple if there are no pairwise crossings among the collection, and no self-crossings.*

If a multicurve is not simple, there are two ways to resolve a crossing so that we obtain a multicurve that no longer contains that crossing. This process is known as *smoothing*:

Definition 4.3. *Let γ, γ_1 , and γ_2 be generalized arcs or closed loops such that we have one of the following two cases:*

- (1) γ_1 crosses γ_2 at a point c , or
- (2) γ has a self-crossing at a point c .

Then we let C be the multicurve $\{\gamma_1, \gamma_2\}$ or $\{\gamma\}$ depending on which of the two cases we are in. We define the smoothing of C at the point x to be the pair of configurations C_+ and C_- . The multicurve C_+ (respectively, C_-) is the same as C except for the local change that replaces the (self-)crossing \times with the pair of segments \cup (resp., \cap). See Fig. 16.



FIGURE 16. Skein relation for ordinary arcs

Theorem 4.4 ([MW13, Props. 6.4, 6.5, 6.6 and Cor. 6.18]). *Let T be a triangulation of a marked surface, with or without punctures. Let C, C_+, C_- be as in Definition 4.3. Then we have the following identity in $\mathcal{A}(B_T)$:*

$$x_C = x_{C_+} + x_{C_-},$$

We now look at an example of resolving a crossing using skein relations.

Example 4.5. *Consider the generalized arc $\gamma(2, 9)$ in the annulus following the notation of Remark 2.14. Using skein relations, we get that the Laurent polynomial $x(\gamma(2, 9))$ corresponding to $\gamma(2, 9)$ is the sum*

$$x(\gamma(4, 7)) + x(\gamma(2, 4))x(\text{Brac}_1).$$

See Fig. 17.

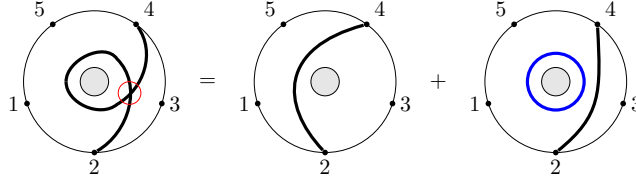


FIGURE 17. Resolving a self-crossing.

The proof that the generalized (ordinary) arcs form an infinite frieze pattern now follows easily from the skein relation.

Proof of Theorem 4.1. Let Bd be a boundary component of a once-punctured disk or an annulus, drawn as a strip. We construct an array \mathcal{F} corresponding to the set of all generalized arcs that are peripheral on Bd as follows. The entries of \mathcal{F} are indexed by (i, j) , $i \leq j \in \mathbb{Z}$ such that our labeling convention is the same as in Definition 3.1.

Set the entry at (i, i) to be 0. Now for every entry at (i, j) , $i < j$, we consider the (generalized) peripheral arc $\gamma(i, j)$ defined by taking the appropriate arc attached to the bottom boundary of the infinite strip \mathcal{U} and projecting this down to the once-punctured disk or annulus. Here, $i, j \in \mathbb{Z}_{\geq 0}$ so the marked points on the boundary Bd are labeled as $(i \bmod n)$ and $(j \bmod n)$. We let the entry at (i, j) of \mathcal{F} be the Laurent polynomial $x(\gamma(i, j))$ corresponding to the generalized arc $\gamma(i, j)$ (see Definition 2.22). Note that $\gamma(i, i+1)$ is a boundary edge, so $x(\gamma(i, i+1)) = 1$ by definition.

To show that \mathcal{F} is a frieze pattern, we need to check that for every diamond

$$\begin{array}{ccc} & b & \\ a & & d \\ & c & \end{array}$$

in \mathcal{F} , the equation $ad - bc = 1$ is satisfied.

From the labeling convention, every diamond in \mathcal{F} has indices of the form

$$\begin{array}{ccc} & (i+1, i+m) & \\ (i, i+m) & & (i+1, i+m+1) \\ & (i, i+m+1) & \end{array}$$

where $m \in \mathbb{Z}_{\geq 1}$. We want to show that

$$x(\gamma(i, i+m)) x(\gamma(i+1, i+m+1)) = 1 + x(\gamma(i+1, i+m)) x(\gamma(i, i+m+1)).$$

Consider the arcs $\gamma(i, i+m), \gamma(i+1, i+m+1)$ drawn in the universal cover of our surface (Fig. 18, top). The arcs $\gamma(i, i+m), \gamma(i+1, i+m+1)$ have exactly one crossing point. Using the skein relations (Theorem 4.4), we have that

$$\begin{aligned} x(\gamma(i, i+m)) x(\gamma(i+1, i+m+1)) &= x(\gamma(i, i+1)) x(\gamma(i+m, i+m+1)) \\ &\quad + x(\gamma(i+1, i+m)) x(\gamma(i, i+m+1)) \\ &= 1 + x(\gamma(i+1, i+m)) x(\gamma(i, i+m+1)). \end{aligned}$$

This holds for every diamond in our pattern, and thus we have constructed a frieze pattern of Laurent polynomials corresponding to the set of all generalized peripheral arcs of Bd . \square

5. PROGRESSION FORMULAS

In Section 4, we constructed infinite frieze patterns of Laurent polynomial entries. In this section, we present formulas governing relations among these entries. These generalize the relations given in [BFPT16], in the sense that [BFPT16, Thm. 2.5] is a special case of the formulas.

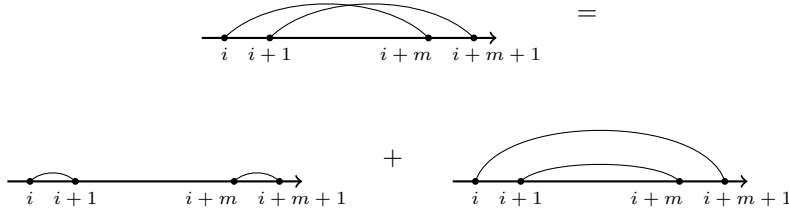


FIGURE 18. Applying skein relations to prove Theorem 4.1

5.1. Complementary arcs. For $1 \leq i, j \leq n$ and $k = 1, 2, \dots$, we let $\gamma_k(i, j)$ denote the generalized peripheral arc in $C_{n,m}$ or D_n that lifts to the covering by the strip as follows (using the notation of Remark 2.14):

$$\gamma_k(i, j) = \begin{cases} \gamma(i, j + (k - 1)n) & \text{if } i < j \\ \gamma(i, j + kn) & \text{if } i \geq j \end{cases}.$$

That is, $\gamma_k(i, j)$ is the generalized peripheral arc that starts at marked point i and finishes at the marked point j (possibly with $i = j$) with $(k - 1)$ self-crossings such that the boundary Bd is to the right of the curve as we trace it.

Definition 5.1 (complementary arc). *Using the above shorthand notation, we define the arc complementary to $\gamma_k = \gamma_k(i, j)$ as*

$$\gamma_k(i, j)^C = \begin{cases} \gamma(j, i + kn) & \text{if } i < j \\ \gamma(j, i + (k - 1)n) & \text{if } i \geq j \end{cases}.$$

Remark 5.2. *When $i \neq j$, the complementary arc γ_k^C to $\gamma_k = \gamma_k(i, j)$ can be described as the generalized arc (i.e. up to homotopy) starting at marked point j and finishing at the marked point i and retaining $(k - 1)$ self-crossings while following the orientation of the surface. See Fig. 19. In this case, $(\gamma_k^C)^C = \gamma_k$. On the other hand, when $i = j$, observe that complementation is non-involutive and simply decreases the number of self-intersections by one. For example, we think of the empty arc as the complementary arc of the once-punctured monogon from i to i , and of the once-punctured monogon from i to i as the complementary arc of the loop from i to i which goes around the boundary Bd twice.*

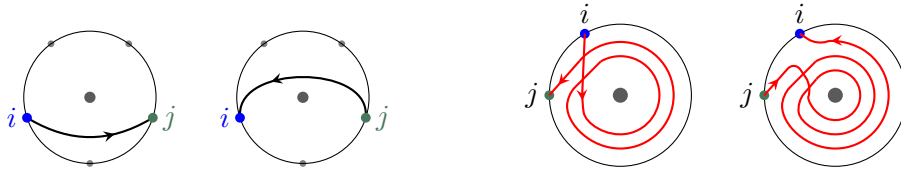


FIGURE 19. Examples of involutive complementary arcs γ_1, γ_1^C and γ_3, γ_3^C .

Remark 5.3. *It is well-known that a finite frieze pattern has glide-symmetry. In an infinite frieze pattern \mathcal{F} , we do not have glide-symmetry, but instead we have what we call complement-symmetry along with the translation-symmetry. See Fig. 20 for an example. Note that each kn -th row ($k \in \mathbb{Z}_{\geq 1}$) of \mathcal{F} corresponds to the generalized arcs of the form $\gamma_k(i, i)$ for which complementation is not involutive.*

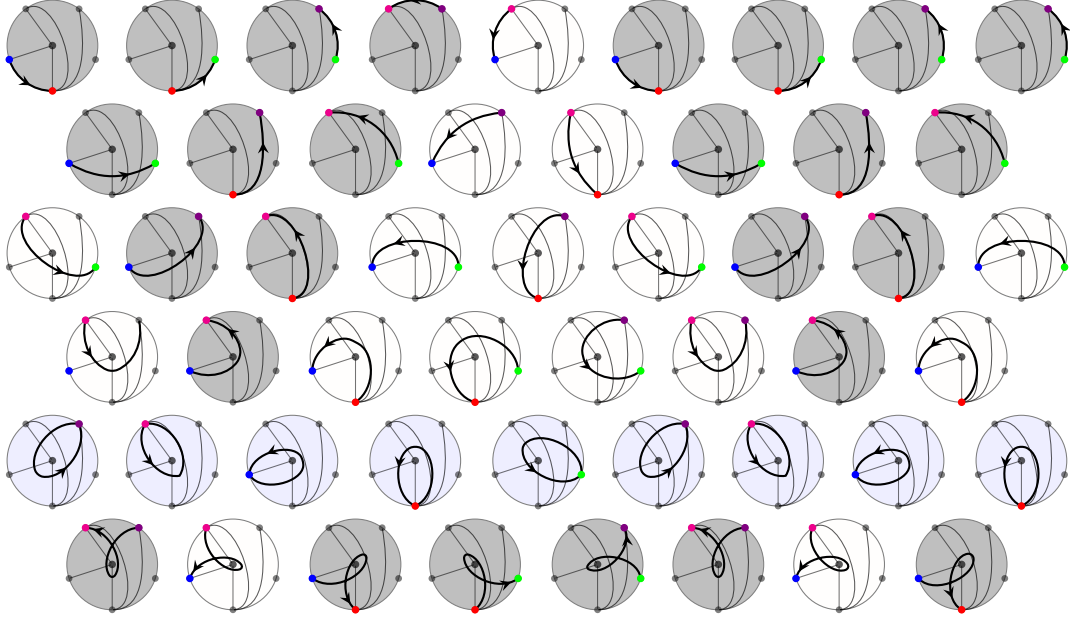


FIGURE 20. An infinite frieze of elements of the cluster algebra corresponding to peripheral curves in a punctured disk.

Theorem 5.4 (progression formulas). *Let γ_1 be a peripheral arc or a boundary edge of (S, M) starting and finishing at points i and j . For $k = 2, 3, \dots$ and $1 \leq m \leq k - 1$, we have*

$$x(\gamma_k) = x(\gamma_m) x(\text{Brac}_{k-m}) + x(\gamma_{k-2m+1}^C).$$

For $r \geq 0$, γ_{-r}^C is defined to be the curve γ_{r+1} with a kink, so that $x(\gamma_{-r}^C) = -x(\gamma_{r+1})$.

Remark 5.5. *Special cases of above theorem are when $m = 1$ (see Fig. 21) and $m = k - 1$. We have*

$$(5.1) \quad x(\gamma_k) = x(\gamma_1) x(\text{Brac}_{k-1}) + x(\gamma_{k-1}^C),$$

$$(5.2) \quad x(\gamma_k) = x(\gamma_{k-1}) x(\text{Brac}_1) - x(\gamma_{k-2})$$

Compare (5.2) with [BFPT16, Thm. 2.5]. In particular, we use the definition $x(\gamma_{-k+3}^C) = -x(\gamma_{k-2})$ in (5.2).

Furthermore, if γ_1 is the boundary edge between i and $i + 1$, then $x(\gamma_1) = 1$, so, due to (5.1), we have

$$(5.3) \quad x(\text{Brac}_k) = x(\gamma_{k+1}) - x(\gamma_k^C).$$

5.2. Proof of Theorem 5.4. Let $\gamma_k := \gamma_k(i, j)$. We draw γ_k so that it first closely follows the other boundary (or the puncture) and then spirals out.

In the covering via the infinite horizontal strip, we draw the lower boundary Bd so that i is drawn to the left of j in each frame. We draw each representative of γ_k as follows. We start at a frame Reg_0 . Starting from a vertex labeled i , our pencil goes north, passing through all of the $(k - 1)$ crossings. When we get to the very north, we turn southeast, and finish at a vertex labeled j , which is located in the frame $k - 1$ frames (respectively, k frames) east of Reg_0 if $i \neq j$ (respectively, if $i = j$). See Fig. 22.

We order the crossings of γ_k so that the first crossing is the one closest to Bd and the $(k - 1)$ -th crossing is the one furthest away from Bd . In each frame, consider the m -th crossing c of γ_k . Denote

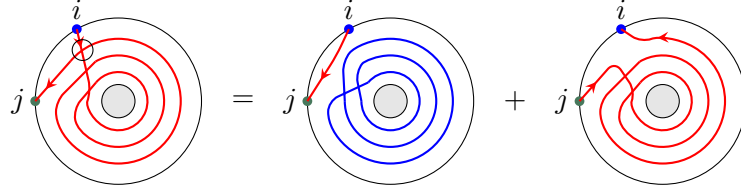


FIGURE 21. Case $m = 1$: By the progression formula (Theorem 5.4), we have $x(\gamma_4) = x(\gamma_1)x(\text{Brac}_3) + x(\gamma_3^C)$.

the segments meeting at c by $north_c$, $south_c$, $east_c$, and $west_c$, so that $north_c$ is the segment drawn north of c , $east_c$ is the segment drawn east of c , et cetera.

If we resolve all representatives of the m -th crossing c by glueing $north_c$ with $west_c$ as well as glueing $south_c$ with $east_c$, we get two curves, γ_m and Brac_{k-m} (see Fig. 23). This explains the first summand of Theorem 5.4. The second summand (see Figs. 24 and 25) of Theorem 5.4 is explained by the following Lemma.

Lemma 5.6. *Suppose we have the same setup as above for γ_k . Suppose we resolve all representatives of the m -th crossing c by glueing $north_c$ with $east_c$ as well as glueing $south_c$ with $west_c$. Then we get one curve, γ_{k-2m+1}^C . See Figs. 24 and 25.*

Proof of Lemma 5.6. Our pencil starts at Reg_0 at the starting vertex i and heads north. Let c_0 denote the m -th crossing of γ_k at frame Reg_0 . When we get to c_0 , since the segment $south_{c_0}$ is glued to $west_{c_0}$, we pivot west of c_0 . As we trace $west_{c_0}$ with our pencil, we pass through $(k-m)$ other frames west of Reg_0 , denoted $\text{Reg}_{-1}, \dots, \text{Reg}_{-(k-m)}$. When we get to $\text{Reg}_{-(k-m)}$, the curve bends south (because this is how we've chosen to draw γ_k). As our pencil traces south, we hit the m -th crossing c' in $\text{Reg}_{-(k-m)}$. Because we have glued $north_{c'}$ with $east_{c'}$, the curve bends east at c' .

Since this crossing is the m -th crossing closest to Bd , there are $m-1$ (possibly $m-1=0$) other crossings beneath it closer to Bd . Therefore, our pencil will end (at a representative of the vertex j) when we get to the frame that is $m-1$ frames (respectively, m frames) away east of $\text{Reg}_{-(k-m)}$ if $i \neq j$ (respectively, if $i = j$).

We consider the two possibilities: $k-m > m-1$ or $k-m \leq m-1$. First, assume $k-m > m-1$. If $i \neq j$, we end at the frame $\text{Reg}_{-(k-m)+(m-1)} = \text{Reg}_{-(k-2m+1)}$, which we have passed earlier. Hence we have traced the curve γ_{k-2m+1}^C (see Fig. 24). If $i = j$, we end at the frame $\text{Reg}_{-(k-m)+m} = \text{Reg}_{-(k-2m)}$, which we have passed earlier. Since we started at Reg_0 , and since $i = j$, we have traced the curve γ_{k-2m} . (In particular, if $k = 2m$, then we have traced a curve that is contractible to the point i). By definition, this curve is γ_{k-2m+1}^C .

If $k-m \leq m-1$, we pass Reg_0 , crossing our pencil mark exactly once before continuing to another frame east of Reg_0 . If $i \neq j$, we end our drawing at a frame that is $m-1 - (k-m) = -k+2m-1$ frames away east of Reg_0 . (In the case $k-m = m-1$, this quantity is zero and indeed we end at the original frame Reg_0 , and we cross our pencil mark exactly once before ending at j .) Denote this frame $\text{Reg}_{(-k+2m-1)}$. Hence we have traced the curve $\gamma_{(-k+2m)}$ with a kink (note that $-k+2m \geq 1$) in this case). By definition, this curve is γ_{k-2m+1}^C (see Fig. 25). If $i = j$, we end our drawing at a frame that is $m - (k-m) = -k+2m$ frames away east of Reg_0 . Denote this frame $\text{Reg}_{(-k+2m)}$. Hence we have traced the curve $\gamma_{(-k+2m)}$ with a kink. By definition, this curve is γ_{k-2m+1}^C . \square

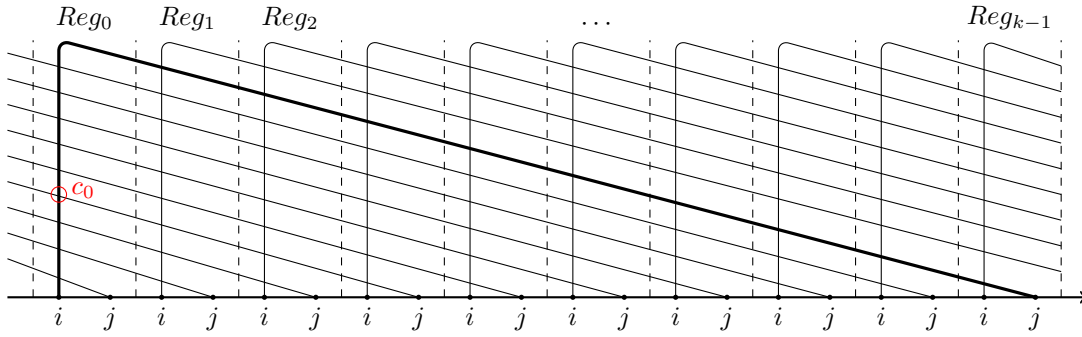


FIGURE 22. Lift of γ_k for $k = 10, m = 4$ drawn on the strip.

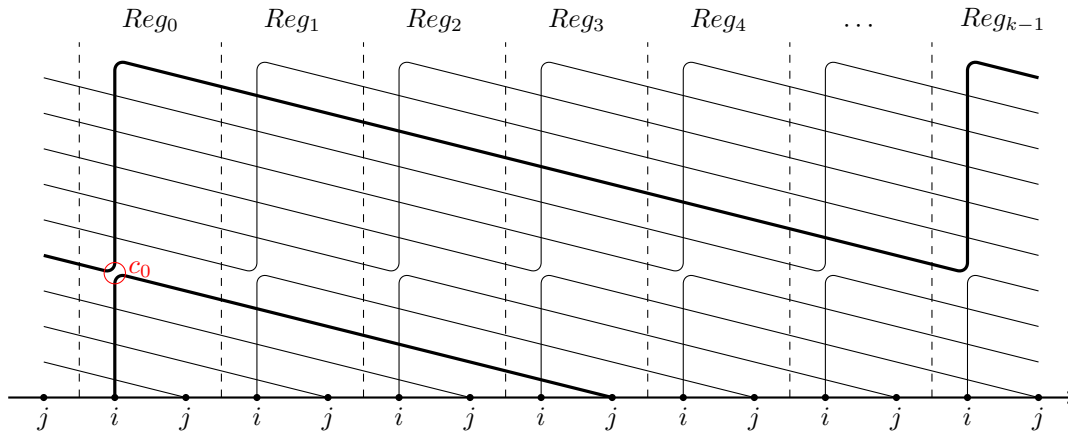


FIGURE 23. Lifts of γ_m and $Brac_{k-m}$ for $k = 10, m = 4$ drawn on the strip.

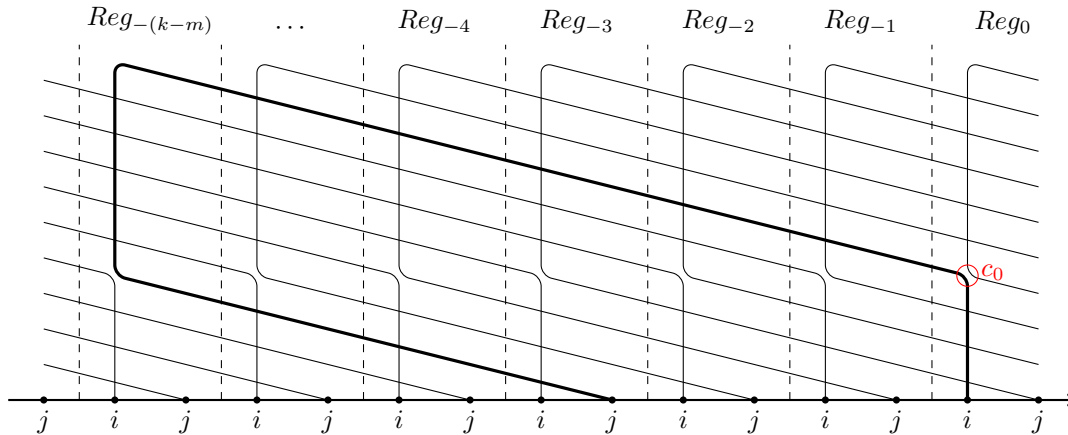


FIGURE 24. Lift of γ_{k-2m+1}^C for $k = 10, m = 4$ drawn on the strip.

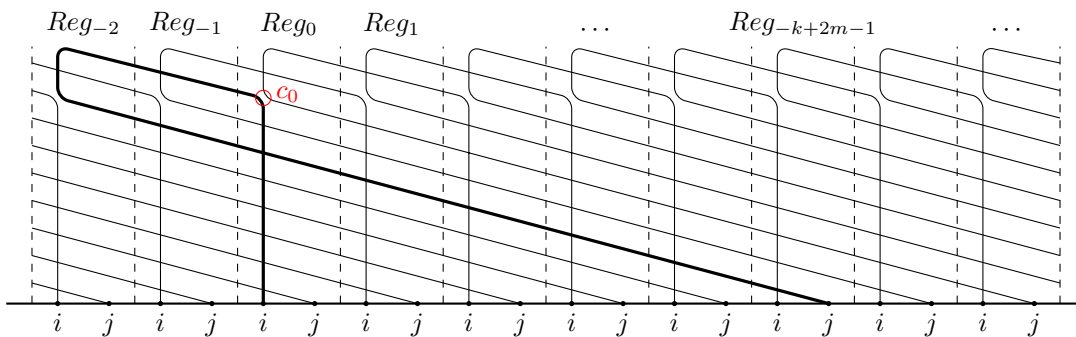


FIGURE 25. Lift of γ_{k-2m+1}^C for $k = 10, m = 8$ drawn on the strip.

6. BRACELETS AND GROWTH COEFFICIENTS

In [BFPT16, Thm. 2.2], the authors show that in an n -periodic infinite frieze of positive integers, the difference between the entries in rows $(nk + 1)$ & $(nk - 1)$ and the same column is a constant. These differences are also constant in our infinite friezes of Laurent polynomials, and we give geometric interpretations to these differences. Following [BFPT16, Def. 2.3], we refer to these constants as *growth coefficients*.

6.1. Growth coefficients. We say that *level k* of a frieze consists of the entries of the frieze indexed by $(i, i + (k - 1)n + j)$ where $j = 1, \dots, n$, that is, the entries in the $(k - 1)n + j$ -th row of the frieze. Compare the following proposition with [BFPT16, Thm. 2.2].

Proposition 6.1. *Let $\mathcal{F} = \{\mathcal{F}_{i,j}\}$ be an infinite periodic frieze pattern as described in Section 4. For each $k \geq 1$, we have*

$$x(\text{Brac}_k) = \mathcal{F}_{i,i+1+kn} - \mathcal{F}_{i+1,i+kn}$$

for all $i \in \mathbb{Z}$.

Proof. Let Bd be the boundary corresponding to \mathcal{F} , with n marked points. Let $i \in \mathbb{Z}$ and suppose that γ_1 is the boundary edge from i to $i + 1$ (taken modulo n). Since $x(\gamma_1) = 1$, due to (5.3), we have

$$x(\text{Brac}_k) = x(\gamma_{k+1}) - x(\gamma_k^C).$$

Observe that γ_{k+1} corresponds to the entry at position $(i, i + 1 + kn)$ and γ_k^C corresponds to the entry at position $(i + 1, i + kn)$. Hence

$$x(\gamma_{k+1}) - x(\gamma_k^C) = \mathcal{F}_{i,i+1+kn} - \mathcal{F}_{i+1,i+kn}.$$

□

Definition 6.2. *Let $\mathcal{F} = \{\mathcal{F}_{i,j}\}$ be an infinite periodic frieze pattern as described in Section 4. Let n be the number of marked points on the outer boundary of the associated triangulated surface. For $k \geq 0$, the k th growth coefficient for \mathcal{F} is given by $s_0 := 2$, and $s_k := \mathcal{F}_{i,i+1+kn} - \mathcal{F}_{i+1,i+kn}$, otherwise.*

Note that s_k measures the difference between entries in the first row of the $(k + 1)$ st level and the penultimate row of the k th level.

Remark 6.3. *Per Proposition 6.1, $s_k = x(\text{Brac}_k)$ whenever $k \geq 1$, so we can use the two terms interchangeably.*

To see that $s_0 = 2$ makes sense in the frieze, see Fig. 26. We write in the row of 0s and then add a row of -1s above the row of 0s. Then $s_0 = 1 - (-1) = 2$.

Given a triangulation of an annulus, we may get two different quiddity sequences q and \bar{q} from the outer and inner boundaries, respectively. We see that $s_q = s_{\bar{q}}$ since Brac_k is defined independently of the choice of the boundary of an annulus. This agrees with [BFPT16, Thm. 3.4].

Remark 6.4. *The progression formulas (Theorem 5.4) give us a way to compute entries on lower levels using the growth coefficients and entries on previous levels. Define $m(\gamma)$ to be the integer obtained from $x(\gamma)$ by specializing all the x_{τ_i} to 1. We demonstrate (5.1) on the frieze pattern of positive integers in Fig. 27. Consider the underlined entry 5 (in the dotted circle) on the first column, which corresponds to the γ_2 for some boundary edge γ_1 . This 5 is equal to $s_1 m(\gamma_1) + m(\gamma_1^C) = 3(1) + 2$. Similarly, we compute the underlined entry 19 =: $m(\gamma_3)$ which is equal to $s_2 m(\gamma_1) + m(\gamma_2^C) = 7(2) + 5$. We can do this for every entry in a frieze pattern.*

$$\begin{aligned}
 T_0(x) &= 2 \\
 T_1(x) &= x \\
 T_2(x) &= x^2 - 2 \\
 T_3(x) &= x^3 - 3x \\
 T_4(x) &= x^4 - 4x^2 + 2 \\
 T_5(x) &= x^5 - 5x^3 + 5x^2 \\
 T_6(x) &= x^6 - 6x^4 + 9x^2 - 2
 \end{aligned}$$

TABLE 1. The normalized Chebyshev polynomials $T_k(x)$ for small k .

recurrence

$$T_k(x) = xT_{k-1}(x) - T_{k-2}(x).$$

Note that $T_k(x)$'s can also be written as $2\text{Cheb}_k(x/2)$, where $\text{Cheb}_k(x)$ denotes the usual Chebyshev polynomial of the first kind, which satisfies $\text{Cheb}_k(\cos x) = \cos(kx)$.

Table 1 shows the first few normalized Chebyshev polynomials. The elements associated to the bracelets (Definitions 2.17 and 2.25) satisfy the normalized Chebyshev polynomials.

Proposition 6.7 ([MSW13, Prop. 4.2]). *We have*

$$x_{\text{Brac}_k} = T_k(x_{\text{Brac}_1}).$$

The recurrence implied by Propositions 6.6 and 6.7 agrees with that of growth coefficients, $s_{k+2} = s_1 s_{k+1} - s_k$ for $k \geq 0$, from [BFPT16, Prop. 2.10].

Remark 6.8. *Suppose Brac_1 is a closed loop without self-crossings enclosing a single puncture. Since $x_{\text{Brac}_1} = 2$ (per Definition 2.25(2)), $T_k(2) = 2$ for all $k \geq 0$ (per Proposition 6.6), and $x_{\text{Brac}_k} = T_k(x_{\text{Brac}_1})$ (per Proposition 6.7), we have*

$$x_{\text{Brac}_k} = 2 \text{ for all } k \geq 0.$$

In particular, if (S, M) is a once-punctured disk, all bracelets are associated to 2, thought of as a scalar in the cluster algebra $\mathcal{A} = \mathcal{A}(S, M)$.

7. RECURSIVE RELATIONSHIPS

7.1. Differences from complement symmetry. We consider the difference between frieze entries associated to complementary arcs of two marked points. For the once-punctured disk, this difference is constant across all levels and is determined by the two marked points. For the annulus, this difference is determined by the level as well as the end points. Recall from Definition 6.2, that $s_k := \mathcal{F}_{i, i+1+kn} - \mathcal{F}_{i+1, i+kn}$ is the k th growth coefficient of a frieze $\mathcal{F} = \{\mathcal{F}_{i,j}\}$.

Proposition 7.1. *Let \mathcal{F} be a frieze pattern coming from a triangulation of a once-punctured disk or annulus. Let $\gamma_1 = \gamma$ be an ordinary arc from i to j (possibly $i = j$) or a boundary edge from i to $i + 1$. Define $c_{k,\gamma} := x(\gamma_k) - x(\gamma_k^C)$. We write $c_k := c_{k,\gamma}$, since γ is understood. Then we have the following relations for $k > 1$:*

- (1) $c_k = (s_{k-1} - s_{k-2})c_1 + c_{k-2}$, where we define $c_0 = c_1$;
- (2)

$$c_k = \begin{cases} c_1 \left(1 + \sum_{i=0}^{k-1} (-1)^{i+1} s_i \right) & \text{for } k \text{ even, and} \\ c_1 \left(1 + \sum_{i=1}^{k-1} (-1)^i s_i \right) & \text{for } k \text{ odd,} \end{cases}$$

where $c_1 = x(\gamma_1) - x(\gamma_1^C)$ is computed from the triangulation or the frieze.

Note that in the case of the once-punctured disk, since $s_k = 2$ for all k , the formula reduces to $c_k = c_1$ for all $k > 1$. Note also that, if $i = j$, then $c_1 = x(\gamma_1)$.

Proof. First, we show that $c_2 = (s_1 - s_0)c_1 + c_0$. Per (5.1), we have $\gamma_2 = s_1 x(\gamma_1) + x(\gamma_1^C)$. We also have $\gamma_2^C = s_1 x(\gamma_1^C) + x(\gamma_1)$ due to (5.1) if $i \neq j$ and due to the fact that $\gamma_2^C = \gamma_1$ and $x(\gamma_1^C) = 0$ if $i = j$. Subtracting the two equations gives us

$$\begin{aligned} c_2 &= x(\gamma_2) - x(\gamma_2^C) = s_1 (x(\gamma_1) - x(\gamma_1^C)) - (x(\gamma_1) - x(\gamma_1^C)) \\ &= s_1 c_1 - c_1 \\ &= (s_1 - 2)c_1 + c_1 \\ &= (s_1 - s_0)c_1 + c_0, \end{aligned}$$

where the last equality is due to the fact that $s_0 = 2$ and $c_0 = c_1$.

If $k \geq 3$, per (5.1), we have $\gamma_k = s_{k-1} x(\gamma_1) + x(\gamma_{k-1}^C)$ and $x(\gamma_{k-1}^C) = s_{k-2} x(\gamma_1^C) + x(\gamma_{k-2})$. Note that the second equation holds even for the case where $i = j$, due to the fact that $\gamma_{k-1}^C = \gamma_{k-2}$ and $x(\gamma_1^C) = 0$ if $i = j$. So $x(\gamma_k) = s_{k-1} x(\gamma_1) + s_{k-2} x(\gamma_1^C) + x(\gamma_{k-2})$. We get a similar equation $x(\gamma_k^C) = s_{k-1} x(\gamma_1^C) + s_{k-2} x(\gamma_1) + x(\gamma_{k-2}^C)$. Subtracting the two gives us (1).

Part (2) is proved by induction. For $k = 1$, we get that $c_1 = c_1$, and for $k = 2$, $c_2 = (s_1 - s_0)c_1 + c_0 = (s_1 - s_0)c_1 + c_1 = c_1 ((-1)^2 s_1 + (-1)^1 s_0 + 1) = c_1 \left(\sum_{i=0}^1 (-1)^{i+1} s_i + 1 \right)$ by (1). Assume (2) holds for some n . If n is even, then $n + 1$ is odd, and

$$\begin{aligned} c_{n+1} &= (s_n - s_{n-1})c_1 + c_{n-1} \text{ by (1)} \\ &= c_1 ((-1)^n s_n + (-1)^{n-1} s_{n-1}) + c_1 \left(\sum_{i=1}^{n-2} (-1)^i s_i + 1 \right) \\ &= c_1 \left(1 + \sum_{i=1}^n (-1)^i s_i \right). \end{aligned}$$

Similarly, if n is odd, then $n + 1$ is even, and we have

$$\begin{aligned} c_{n+1} &= (s_n - s_{n-1})c_1 + c_{n-1} \text{ by (1)} \\ &= c_1 ((-1)^{n+1} s_n + (-1)^n s_{n-1}) + c_1 \left(\sum_{i=0}^{n-2} (-1)^{i+1} s_i + 1 \right) \\ &= c_1 \left(\sum_{i=0}^n (-1)^{i+1} s_i + 1 \right). \end{aligned}$$

Thus the result holds true for all n . □

7.2. Arithmetic progressions. Friezes coming from triangulations of once-punctured disks satisfy a beautiful arithmetic property. Consider the frieze \mathcal{F}_T in Fig. 28, where T is a triangulation of D_5 ; when jumping 5 steps along any diagonal in \mathcal{F}_T , we get a sequence of numbers that with a *common difference*. Thus these sequences of numbers form an increasing arithmetic progression (see Def. 3.10 of [Tsc15]). The dotted and dashed circles in Fig. 28 show examples of two 5-arithmetic progressions in the frieze.

Theorem 7.2 ([Tsc15, Thm. 3.11]). *Every n -periodic infinite frieze \mathcal{F}_T associated to a triangulation T of D_n is n -arithmetic.*

The following is an analog of Theorem 7.2.

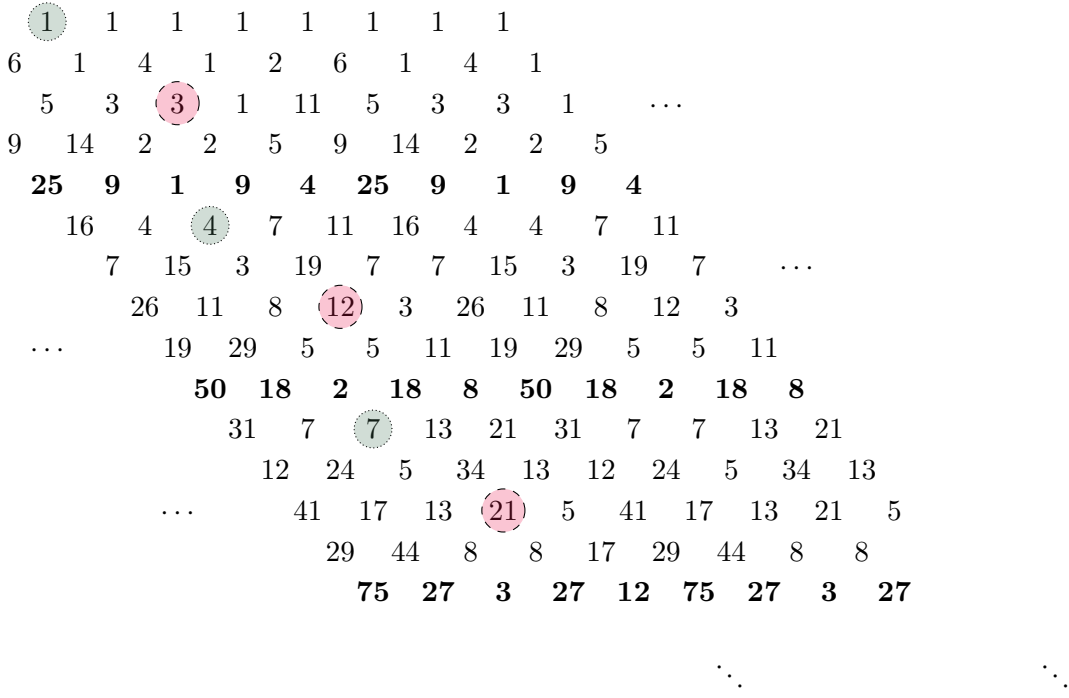


FIGURE 28. Arithmetic progression in a frieze. The dotted and dashed circles show two different arithmetic progressions. The dotted circles have a common difference of 3, the dashed circles of 9.

Proposition 7.3 (Corollary of Theorem 5.4). *Suppose (S, M) is a once-punctured disk. Let $\gamma_1 = \gamma$ be an ordinary arc from i to j (possibly $i = j$) or a boundary edge from i to $i + 1$. Then, for $k \geq 2$, we have*

$$x(\gamma_k) = x(\gamma_{k-1}) + (x(\gamma_1) + x(\gamma_1^C))$$

Proof of proposition 7.3. We prove this by induction on k .

First, we have

$$\begin{aligned} x(\gamma_2) &= x(\text{Brac}_1) x(\gamma_1) + x(\gamma_1^C) \text{ by (5.1)} \\ &= 2 x(\gamma_1) + x(\gamma_1^C) \text{ by Remark 6.8} \\ &= x(\gamma_1) + (x(\gamma_1) + x(\gamma_1^C)). \end{aligned}$$

Similarly, $x(\gamma_2^C) = x(\gamma_1^C) + (x(\gamma_1) + x(\gamma_1^C))$. (Note that, if $i = j$, we have $x(\gamma_2^C) = x(\gamma_1)$ and $x(\gamma_1^C) = 0$, and so these expressions for $x(\gamma_2)$ and $x(\gamma_2^C)$ are still valid in this case.)

Next, suppose by induction we have the equality $x(\gamma_k) = x(\gamma_{k-1}) + (x(\gamma_1) + x(\gamma_1^C))$ as well as $x(\gamma_k^C) = x(\gamma_{k-1}^C) + (x(\gamma_1) + x(\gamma_1^C))$, where again we let $x(\gamma_1^C) = 0$ if $i = j$. Then

$$\begin{aligned} x(\gamma_{k+1}) &= 2 x(\gamma_1) + x(\gamma_k^C) \text{ by (5.1) and Remark 6.8} \\ &= 2 x(\gamma_1) + x(\gamma_{k-1}^C) + (x(\gamma_1) + x(\gamma_1^C)) \text{ by the inductive hypothesis} \\ &= x(\gamma_k) + (x(\gamma_1) + x(\gamma_1^C)) \text{ by (5.1) and Remark 6.8.} \end{aligned}$$

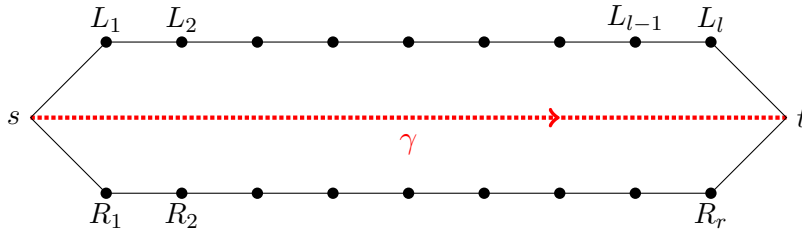
□

APPENDIX A. A BIJECTION BETWEEN BCI TUPLES AND T-PATHS

It is known that a combinatorial T -path formula can be used to compute the Laurent expansion for an arc in a polygon [Sch08a] (see also [ST09, GM15] for the case of a general surface). On the other hand, every entry in a finite (respectively, infinite) integral frieze counts the number of matchings, m_{ij} , between vertices of a polygon (respectively, once-punctured disk or annulus) and triangles of the associated triangulation [BCI74, Section 2] (respectively, [Tsc15, Section 4.5] and [BPT16, Section 5]). We give a bijection between these classical matching tuples and the more recent T -paths. In the case of polygons, such a bijection was constructed by Carroll and Price [CP03, Pro05] in unpublished work. This gives a combinatorial formula (Corollary A.8) for computing Laurent expansion formulas for cluster variables via these matching tuples in the case of a once-punctured disk or an annulus.

Throughout this section, let T be a triangulation of an annulus or a once-punctured disk (S, M) . Let γ be a generalized peripheral arc (allowing self-crossings) on a boundary component Bd of (S, M) .

Choose the usual orientation so that Bd is to the right of γ . For the purpose of computing the Laurent polynomial expansion of $x(\gamma)$, we will work with a finite polygon cover \tilde{S}_γ of T containing a lift of γ . By abuse of notation, we also denote the lift of γ in \tilde{S}_γ by γ . Let s and t be the starting and ending points of γ , respectively. Let R_1, R_2, \dots, R_r be the boundary vertices to the right of γ , not including s and t , and let L_1, \dots, L_l be the boundary vertices to the left of γ . These vertices are ordered so that $s, R_1, R_2, \dots, R_r, t, L_1, \dots, L_2, L_1$ go counterclockwise around the polygon cover \tilde{S}_γ . See Figures 29 and 30. We say that the R_i are the right vertices and the L_i are the left vertices.

FIGURE 29. A generic polygon cover for a generalized arc γ .A.1. BCI tuples and T -paths.

Definition A.1 ([BCI74, Section 2]). A BCI tuple for γ is an r -tuple (t_1, \dots, t_r) such that:

- (B1) the i -th entry t_i is a triangle of \tilde{S}_γ having R_i as a vertex. (We say that the vertex R_i is matched to the triangle in the i -th entry of the tuple, and write $\Delta(R_i) := t_i$).
- (B2) the entries are pairwise distinct.

Let $\Delta_0, \dots, \Delta_d$ be the triangles of \tilde{S}_γ which are crossed by γ , in order.

Example A.2. The following are the BCI tuples for the generalized arc γ from Fig. 30. Note that A, B, C, D, E , and F are the triangles which are not crossed by γ but which are adjacent to at least one of the vertices R_1, \dots, R_8 (located to the right of γ).

- i.* $(\Delta_3, A, B, C, D, \Delta_4, E, F)$
- ii.* $(\Delta_2, A, B, C, D, \Delta_5, E, F)$
- iii.* $(\Delta_2, A, B, C, D, \Delta_4, E, F)$
- iv.* $(\Delta_2, A, B, C, D, \Delta_3, E, F)$
- v.* $(\Delta_1, A, B, C, D, \Delta_5, E, F)$
- vi.* $(\Delta_1, A, B, C, D, \Delta_4, E, F)$
- vii.* $(\Delta_1, A, B, C, D, \Delta_3, E, F)$
- viii.* $(\Delta_0, A, B, C, D, \Delta_5, E, F)$

- ix.* $(\Delta_0, A, B, C, D, \Delta_4, E, F)$
- x.* $(\Delta_0, A, B, C, D, \Delta_3, E, F)$
- xi.* $(\Delta_3, A, B, C, D, \Delta_5, E, F)$

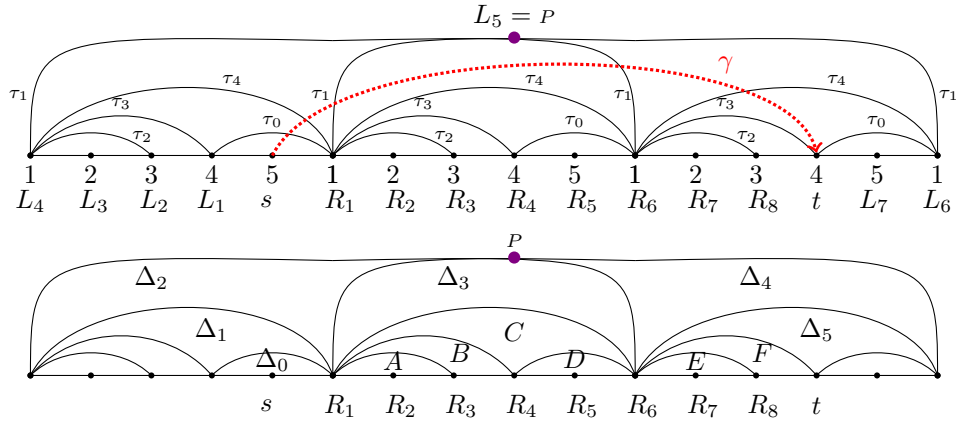


FIGURE 30. Finite polygon cover of T containing copies of triangles crossed by a lift of γ .

Definition A.3 (BCI trail). Let b be a BCI tuple for γ . We define $\text{trail}(b) := \alpha = (\alpha_1, \dots, \alpha_{\text{length}(\alpha)})$ to be a walk from the beginning to the ending point of γ along edges of the triangulation \tilde{S}_γ such that:

- (TR i) the triangles in b (called matched triangles) are to the right of α , and
- (TR ii) the triangles not in b (called unmatched triangles) are to the left of α .

For example, Fig. 31 shows $\text{trail}(b) = (b_{40}, \tau_0, \tau_1, \tau_1, \tau_3)$ for a BCI tuple $b = (\Delta_0, A, B, C, D, \Delta_3, E, F)$ from Example A.2.

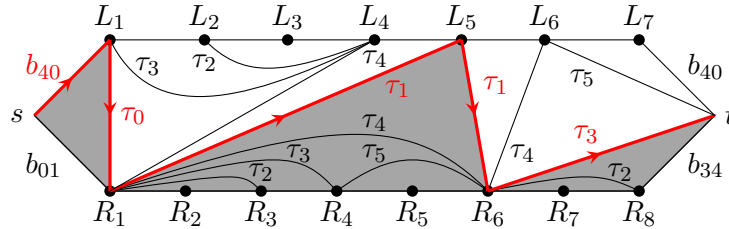


FIGURE 31. The walk $\text{trail}(b) = (b_{40}, \tau_0, \tau_1, \tau_1, \tau_3)$ in \tilde{S}_γ for a BCI tuple $b = (\Delta_0, A, B, C, D, \Delta_3, E, F)$ from Example A.2.

We say that $\text{trail}(b)$ is the BCI trail associated to b . By convention, if γ is an arc of T , the BCI tuple for γ is an empty tuple, and γ is the BCI trail of length 1 for itself.

Remark A.4. To see that Definition A.3 is well-defined, we observe that, if $t_1 \neq \Delta_0$, the first step of α must go along the edge from s to R_1 . Otherwise, the first step goes from s to L_1 . Similarly, the last step of α goes from L_l to t if Δ_d is matched. If R_r is matched to a different triangle, then the last step of α goes from R_r to t . It is clear that no two distinct BCI tuples correspond to the same BCI trail.

Since we are working on a polygonal cover, we only need to recall the definition of (reduced) T -paths of type A. However, T -paths can be defined directly on ideal triangulations of a general marked surface [ST09, Sch10] (possibly a once-punctured disk, see [GM15]).

Definition A.5 ([Sch08a, Definition 1], reduced T -paths). Let T denote the triangulation of \tilde{S}_γ , where τ_1, \dots, τ_d are the inner diagonals, and $\tau_{d+1}, \dots, \tau_{2d+3}$ are the boundary edges of the polygon cover \tilde{S}_γ . A reduced T -path for $\gamma = (s, t)$ is a sequence

$$\alpha = (a_0, a_1, \dots, a_{\text{length}(\alpha)} | i_1, i_2, \dots, i_{\text{length}(\alpha)})$$

such that

- (T1) $s = a_0, a_1, \dots, a_{\text{length}(\alpha)} = t$ are vertices of \tilde{S}_γ .
- (T2) Each τ_{i_k} connects the vertices $a_{i_{k-1}}$ and a_{i_k} for each $k = 1, 2, \dots, \text{length}(\alpha)$.
- (T3) No step goes along the same edge twice.
- (T4) The length of a T -path is odd.
- (T5) Every even step crosses γ .
- (T6) If $j < k$ and both τ_{i_j} and τ_{i_k} cross γ , then the crossing point of τ_{i_j} and γ is closer to the vertex s than the crossing point of τ_{i_k} and γ .

We will show the following in Sections A.3 and A.4.

Proposition A.6. Let γ be a generalized arc. The BCI trail map defined in Definition A.3 gives a bijection between the set of BCI tuples for γ and the set of reduced T -paths for γ .

A.2. Cluster expansion formula in terms of BCI tuples. We assign to a BCI tuple b the same weight as the reduced T -path corresponding to it. This choice of weight agrees with the weighting given by Carroll and Price [CP03] and Propp [Pro05, pages 10-11]. An equivalent weighting is used in a recent article [Yur16, Lemma 4.4].

Definition A.7 (Laurent monomial). To any BCI tuple b , we associate an element $x(b)$ in the cluster algebra $\mathcal{A}(S, M)$ by first considering $\text{trail}(b) = \alpha = (\alpha_1, \dots, \alpha_{\text{length}(\alpha)})$ and setting

$$x(b) = x(\alpha) = \frac{\prod_{i \text{ odd}} x_{\alpha_i}}{\prod_{i \text{ even}} x_{\alpha_i}}.$$

Due to Proposition A.6, we can rewrite the reduced T -path cluster expansion formula [Sch08a, Thm. 1.2] in terms of BCI tuples as follows.

Corollary A.8 (BCI tuple expansion formula). Let $\mathcal{A}(S, M)$ be a cluster algebra arising from (S, M) , as per Theorem 2.11. Let γ be a peripheral generalized arc. The Laurent polynomial corresponding to γ with respect to the cluster x_T is

$$(A.1) \quad x_\gamma = \sum_b x(b)$$

where the sum is over all BCI tuples b for γ . This formula does not depend on our choice of orientation on γ .

Example A.9 (Example of a Laurent expansion corresponding to a generalized arc). Consider the ideal triangulation T of a once-punctured disk and a generalized arc in Fig. 30. We obtain the 11 BCI tuples for γ , listed in Example A.2. Following (A.1), we compute

$$x_\gamma = \frac{x_0 x_1 x_4 + 2x_1 x_3 x_4 + 2x_0^2 + 4x_0 x_3 + 2x_3^2}{x_0 x_1 x_4}$$

by specializing $x(\tau) = 1$ for each boundary edge τ .

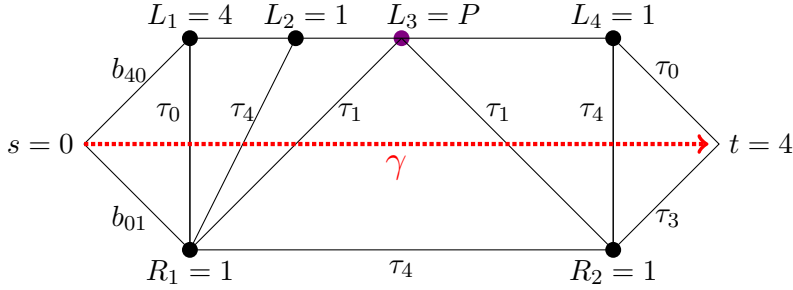


FIGURE 32. Finite $(5 + 3)$ -gon cover \tilde{S}_γ from Fig. 30 (also see Fig. 44).

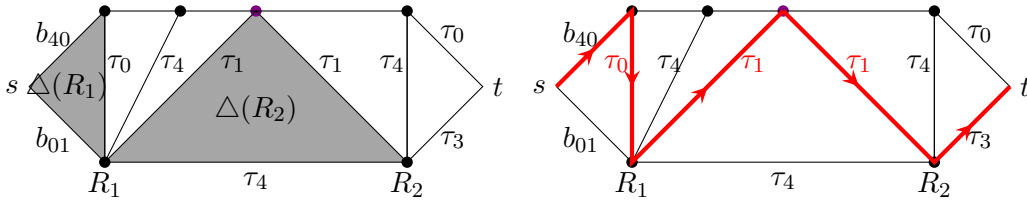


FIGURE 33. A BCI tuple $b = (\Delta_0, \Delta_3)$ for γ and corresponding BCI trail $(b_{40}, \tau_0, \tau_1, \tau_1, \tau_3)$.

A.3. Proof that the trail map sends BCI tuples to T -paths. In this section, we show that the map

$$\begin{aligned} \{\text{BCI tuples for } \gamma\} &\rightarrow \{\text{reduced } T\text{-paths for } \gamma\} \\ b &\mapsto \text{trail}(b), \end{aligned}$$

where $\text{trail}(b)$ is the BCI trail corresponding to b defined in Definition A.3, is well-defined. We mean this in the sense that, given a BCI tuple b for γ , the walk $\text{trail}(b)$ is indeed a reduced T -path for γ .

Lemma A.10. *Suppose that the i -th right vertex R_i is not adjacent to a triangle which crosses γ . Then R_i can only be matched to one triangle, and so the i -th entry in every BCI tuple for γ is fixed.*

Proof. Let b be a BCI tuple for γ . If such a vertex exists, there must be a vertex R_j which is adjacent to exactly one triangle Δ . Then $t_j = \Delta$ by (B1). As in [BCI74, Section 2], we can remove Δ from \tilde{S}_γ and get a smaller triangulated polygon. By induction, we can remove all vertices not adjacent to a triangle crossed by γ this way. \square

Remark A.11. *Due to Lemma A.10, we can assume without loss of generality that all vertices of \tilde{S}_γ are adjacent to triangles crossed by γ . Note that this gives us the same triangulated polygon cover defined in [MSW11, Section 7] (see also an exposition in [GM15, Section 4.1]). Every right vertex R_i is adjacent to at least 2 triangles of \tilde{S}_γ , with the exception of the starting vertex s and the finishing vertex t , which are adjacent to exactly one triangle Δ_0, Δ_d , respectively.*

Fig. 30 illustrates Lemma A.10. The triangles A, B, C, D, E , and F (which do not cross γ) appear in every BCI tuple. Instead of Fig. 30, we work with Fig. 32. When drawing this smaller triangulated polygon cover, we relabel the vertices of \tilde{S}_γ , so that the indices of R and L are consecutively ordered. For example, vertex R_6 in Fig. 30 is now vertex R_2 in Fig. 32. Compare Fig. 31 with Fig. 33.

Lemma A.12. Let $b = (t_1, \dots, t_r) = (\Delta(R_1), \dots, \Delta(R_r))$ be a BCI tuple for γ and let $\alpha = (\alpha_1, \dots, \alpha_{\text{length}(\alpha)})$ be its corresponding BCI trail.

- (1) If α_{2j} goes from a vertex R (to the right of γ) to a vertex L (to the left of γ), then, in the tuple b , R is matched to the triangle which is crossed by γ immediately after α_{2j} .
- (2) If α_{2j} goes from a vertex L (to the left of γ) to a vertex R (to the right of γ), then, in the tuple b , R is matched to the triangle which is crossed by γ immediately before α_{2j} .
- (3) Every even step α_{2j} crosses γ . So we have either situation (1) or (2).
- (4) Furthermore, the length of α is odd.

Proof. We prove (1), (2), and (3) by induction on j . The first step must go from the starting point s of γ to either R_1 (the first vertex to the right of γ) or L_1 (the first vertex to the left of γ).

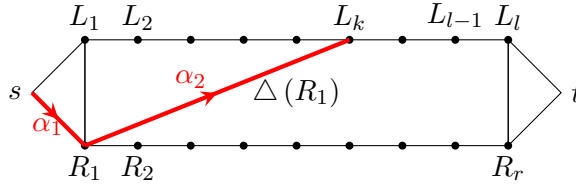


FIGURE 34. The first step α_1 ends at the right vertex R_1 , and α_2 ends at a left vertex L_k for $k \geq 1$ (Lemma A.12 Case 1).

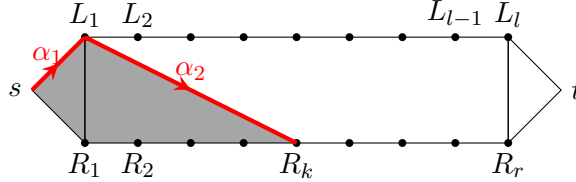


FIGURE 35. The first step α_1 ends at the left vertex L_1 , and α_2 ends at a right vertex R_k for $k \geq 1$ (Lemma A.12 Case 2). Shaded region represents triangles $\Delta_0, \dots, \Delta_{k-1}$.

First, suppose R_1 is not matched to the first triangle Δ_0 crossed by γ . See Fig. 34. Since Δ_0 is not adjacent to other vertices to the right of γ , the BCI tuple b corresponding to α does not contain Δ_0 . Then α_1 must go to R_1 because an unmatched triangle of \tilde{S}_γ has to be to the left of α . Then R_1 is matched to a different triangle t_1 which γ crosses some time after Δ_0 , and no other triangle (if any) between Δ_0 and t_1 is contained in b . Hence, by (TR i) and (TR ii), t_1 is immediately to the right of the next step α_2 . Hence α crosses γ by going from R_1 to a left vertex. This is the base case for (1) and (3).

Second, suppose R_1 is matched to the first triangle Δ_0 crossed by γ . See Fig. 35. Then Δ_0 is the closest matched triangle to s . Then α_1 must go to L_1 because a matched triangle has to be to the right of γ . For some $k \geq 1$ (possibly $k = 1$), the triangles $t_1 = \Delta_0, \dots, t_k = \Delta_{k-1}$ matched by R_1, R_2, \dots, R_k form a maximal connected fan. Then α_2 crosses γ by going from L_1 to R_k . Furthermore, the triangle Δ_{k-1} matched to R_k appears immediately before α_2 . This is the base case for (2) and (3).

Let j be given and assume α_{2j} crosses γ . First, assume (1): suppose α_{2j} starts from a right vertex R and ends at a vertex left L_k , and suppose that the triangle $\Delta(R)$ matched to R appears immediately after α_{2j} . See Figs. 36 and 37.

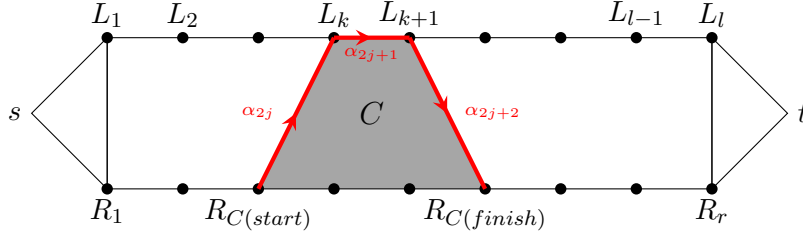


FIGURE 36. The subpath $\alpha_{2j}, \alpha_{2j+1}, \alpha_{2j+2}$ starts and finishes on the right of γ . Lemma A.12 Case 1: When α_{2j} starts at a right vertex and α_{2j+2} ends at a right vertex

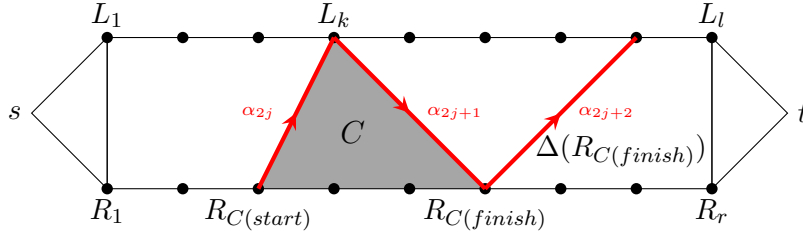


FIGURE 37. The subpath $\alpha_{2j}, \alpha_{2j+1}, \alpha_{2j+2}$ starts on the right and finishes on the left of γ . Lemma A.12 Case 1: α_{2j} starts to the right of γ and α_{2j+2} ends to the left of γ .

If $k = l$, then L_k is the last vertex to the left of γ before the ending point t of γ . Hence the triangles matched to vertices between R and R_r (inclusive) form a maximal connected fan which contains Δ_d . Therefore α_{2j+1} goes from L_l to t , proving (4). So suppose $k < l$.

Consider the maximal connected component C of matched triangles which $\Delta(R)$ is a part of. The edge between L_k and L_{k+1} is an edge of a triangle $\Delta[L_k, L_{k+1}]$. Consider these two possibilities: either $\Delta[L_k, L_{k+1}]$ is in C or it is not. Suppose it is. See Fig. 36. Then α_{2j+1} must go from L_k to L_{k+1} so that the matched triangles stay to the right of α . Furthermore, the right vertex $R_{C(\text{finish})}$ that bounds C on the side that is closest to the end of γ must be matched to a triangle in C . (Note that vertex $R_{C(\text{finish})}$ is isomorphic to R if and only if C contains exactly one triangle, $\Delta(R)$). Also, C cannot include $\Delta[L_{k+1}, L_{k+2}]$. Then α_{2j+2} must go from L_{k+1} to $R_{C(\text{finish})}$ in order to obey Definition A.3. This satisfies (3) for $j + 1$. Furthermore, the triangle which is matched to $R_{C(\text{finish})}$ appears immediately before α_{2j+2} , satisfying (1) for $j + 1$.

Consider the other possibility ($\Delta[L_k, L_{k+1}]$ not in C) as in Fig. 37. If the edge between L_k and L_{k+1} is not an edge of C , then α_{2j+1} must go to a right vertex $R_{C(\text{finish})}$ in order to keep the unmatched triangles to the left of α . But in this situation $R_{C(\text{finish})}$ is not matched to a triangle in C , so $R_{C(\text{finish})}$ must be matched to a triangle $\Delta(R_{C(\text{finish})})$ outside of C . Since by assumption C is a maximal connected component of matched triangles, there must be at least one unmatched triangle immediately after C . Then α_{2j+2} needs to go to a left vertex in order to have the unmatched triangles stay to the left of α and the triangle $\Delta(R_{C(\text{finish})})$ be to the right of α .

Second, assume (2): suppose α_{2j} ends at a vertex R_k (to the right of γ), and suppose that the triangle $\Delta(R_k)$ matched to R_k appears immediately before α_{2j} . See Figs. 38 and 39.

If $k = r$, then R_k is the last vertex before the ending point of γ . Then the rest of the triangles after $\Delta(R_r)$ (if any) are not matched, so they need to be to the left of α , and so α_{2j+1} goes from R_r to t . This proves (4). So suppose $k < r$.

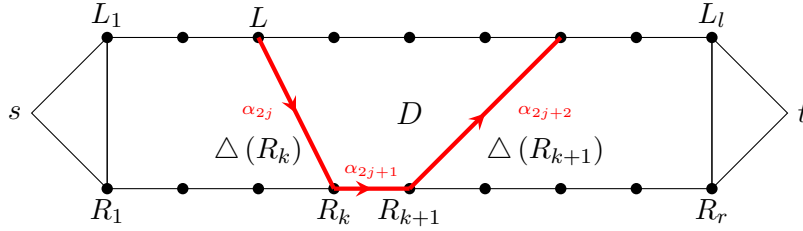


FIGURE 38. The subpath $\alpha_{2j}, \alpha_{2j+1}, \alpha_{2j+2}$ starts and finishes on the left of γ . Lemma A.12 Case 2: α_{2j} starts to the left of γ and α_{2j+2} ends to the left of γ .

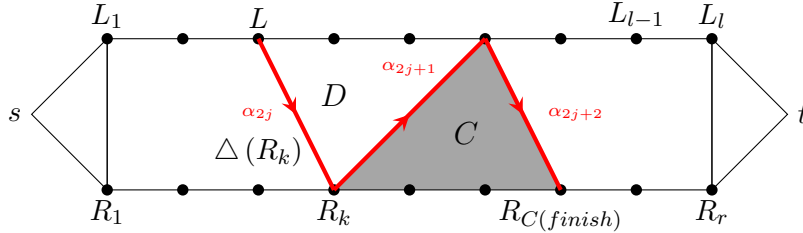


FIGURE 39. The subpath $\alpha_{2j}, \alpha_{2j+1}, \alpha_{2j+2}$ starts on the left and finishes on the right of γ . Lemma A.12 Case 2: When α_{2j} starts to the left of γ and α_{2j+2} ends to the right of γ .

Let D denote the maximal connected component of the unmatched triangles between $\Delta(R_k)$ and $\Delta(R_{k+1})$. Note that D needs to be to the left of α_{2j+1} by (TR ii). If the edge between R_k and R_{k+1} is an edge of D , then α_{2j+1} needs to go from R_k to R_{k+1} . Then α_{2j+2} must go from R_{k+1} to a left vertex (since R_{k+1} must be matched to the triangle adjacent to R_{k+1} which appears immediately after D). See Fig. 38.

If the edge between R_k and R_{k+1} is not an edge of D , then R_{k+1} must be matched to a triangle adjacent to R_k . So α_{2j+1} goes from R_k to a left vertex. See Fig. 39. Let C be the maximal connected fan of matched triangles which contain $\Delta(R_{k+1})$. Every right vertex in C must be matched to a triangle as close to the beginning of γ as possible. Hence this component forms a pyramid shape fan (with the base to the right of γ), and so α_{2j+2} goes from the left of γ to the right of γ . Furthermore, the endpoint of α_{2j+2} is matched to the triangle immediately before α_{2j+2} . This concludes our induction step for (2) and (3). \square

Proposition A.13. *A BCI trail for γ is a reduced T -path for γ .*

Proof. The definition of a BCI trail satisfies (T1), (T2), (T3), and (T6). Lemma A.12 proves that a BCI trail satisfies (T4) and (T5). \square

A.4. Triangles map. Conversely, given a reduced T -path α for γ , we show that the set of triangles to the right of γ forms a BCI tuple for γ . We define the map

$$\begin{aligned} \{\text{reduced } T\text{-paths for } \gamma\} &\rightarrow \{\text{BCI tuples for } \gamma\} \\ \alpha &\mapsto \text{triangles}(\alpha) \end{aligned}$$

which associates to α a tuple of triangles of \tilde{S}_γ that are to the right of α . The following algorithm tells us the well-defined way to match the R_i 's to triangles as we go along \tilde{S}_γ from R_1 to R_r .

If α_1 goes from s to the right vertex R_1 , we assign $\Delta(R_1)$ to be the triangle immediately to the right of α_2 . See Fig. 34.

If α_1 goes to the left vertex L_1 , then α_2 goes from L_1 to some right vertex R_k . We match the first k vertices R_1, \dots, R_k to the triangles $\Delta_0, \dots, \Delta_{k-1}$, in order. These triangles are represented by the shaded area in Fig. 35.

Since α_{2j} must cross γ , this step must go from the right to the left of γ (or vice versa). First, suppose α_{2j} goes from a right vertex $R_{C(start)}$ to some left vertex L_k . Then $R_{C(start)}$ has not been matched yet to any triangle which is crossed by γ prior to α_{2j} .

If α_{2j+1} goes from L_k to the next left vertex L_{k+1} , then α_{2j+2} goes from L_{k+1} to a right vertex $R_{C(finish)}$ where $C(start) \leq C(finish)$ (possibly $C(start) = C(finish)$). We match the vertices $R_{C(start)}, \dots, R_{C(finish)}$ to the triangles in the trapezoid bounded by the subpath $\alpha_{2j}, \alpha_{2j+1}, \alpha_{2j+2}$. See Fig. 36.

If α_{2j+1} goes from L_k to a right vertex $R_{C(finish)}$ where $C(start) < C(finish)$, then we match the vertices $R_{C(start)}, \dots, R_{C(finish)-1}$ to the triangles in the fan bounded by the subpath $\alpha_{2j}, \alpha_{2j+1}, \alpha_{2j+2}$. See Fig. 37.

Second, suppose α_{2j} goes from a left vertex L to some right vertex R_k . Then R_k has been matched to the triangle (having α_{2j} as a side) which is crossed by γ prior to α_{2j} .

If α_{2j+1} goes from R_k to R_{k+1} , then α_{2j+2} goes from the right to the left of γ (see Fig. 38). This situation for α_{2j+2} has been discussed earlier.

If α_{2j+1} goes from R_k to a left vertex and α_{2j+2} goes to a right vertex $R_{C(finish)}$ (where $k < C(finish)$), then we match $R_{k+1}, \dots, R_{C(finish)}$ to the triangles in the fan bounded by the subpath $\alpha_{2j+1}, \alpha_{2j+2}$. See Fig. 39.

Finally, the final (and hence odd) step of α either starts from L_l or from R_r . If the final step goes from L_l to t , then the previous even step finishes at a left vertex (Fig. 37 or 38). Hence R_r has not been matched to a triangle yet. We match R_r to the final triangle Δ_d . If the final step goes from R_r to t , then the previous even step finishes at a right vertex (Fig. 36 or 39). Hence R_r has been matched to the triangle having this even step as a side. By construction, the triangles map is well-defined.

Lemma A.14. *The triangles map $\alpha \mapsto \text{triangles}(\alpha)$ is the inverse of the trail map $b \mapsto \text{trail}(b)$. In particular, both maps are bijections.*

Proof. Let $\alpha = (\alpha_1, \dots, \alpha_{\text{length}(\alpha)})$ be a reduced T -path for γ . Then $\text{triangles}(\alpha)$ are the triangles to the right of α , which form a BCI tuple for γ . But $\text{trail}(\text{triangles}(\alpha))$ is the reduced T -path to the left of $\text{triangles}(\alpha)$, so $\alpha = \text{trail}(\text{triangles}(\alpha))$.

Conversely, let $b = (\Delta(R_1), \dots, \Delta(R_r))$ be a BCI tuple for γ . Then $\text{triangles}(\text{trail}(b))$ is the tuple of all the triangles to the right of $\text{trail}(b)$. Since $\text{trail}(b)$ is the trail to the left of b , we have $b = \text{triangles}(\text{trail}(b))$. \square

A.5. Natural lattice structure of the BCI tuples.

Remark A.15. *It is known that the set of all snake graph perfect matchings has a natural distributive lattice structure [MSW13, Theorem 5.2] (as a consequence of [Pro02, Thm. 2]). Using a bijection of [MS10, Thm. 4.6] between snake graph perfect matchings and complete T -paths (see [Sch10, Def. 2]), it is straight-forward to show that the BCI tuples have a natural lattice structure which is preserved by the bijection of Proposition A.6.*

In the same spirit as [MS10, Sch10, MSW13], we define the minimal (respectively, maximal) BCI tuple to be the tuple where each chosen triangle is as close as possible to (respectively, as far as possible from) the starting point of γ . Recall that, due to the convention we use in Definition 2.9, our convention is equivalent to the convention of [MS10, Sch10], so our choice of the minimal BCI tuple corresponds to the minimal snake graph matching and complete T -path in said articles.

Definition A.16 (Minimal and maximal BCI tuples). *For a vertex R_i to the right of γ , denote by $FAN(R_i)$ the fan of all triangles adjacent to R_i which are crossed by γ . Per Remark A.11, this*

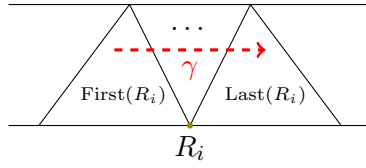


FIGURE 40. The collection $FAN(R_i)$ of triangles adjacent to R_i .

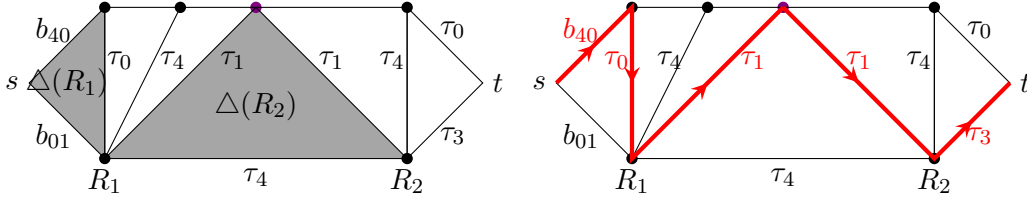


FIGURE 41. The (minimal) BCI tuple $(First(R_1), First(R_2))$ for γ from Figure 32 and its corresponding reduced T -path.

fan contains at least two triangles. See Fig. 40. The orientation of γ determines an ordering of the triangles in this fan. Let $fan(R_i)_k$ be the k -th triangle in $FAN(R_i)$. Let $First(R_i) := fan(R_i)_1$ and $Last(R_i) := fan(R_i)_{|FAN(R_i)|}$ denote the first and last triangles in this fan. We say that a BCI tuple is the minimal BCI tuple if each vertex R_i is mapped to $First(R_i)$ (see Fig. 41). Similarly, the maximal BCI tuple is defined to be $(Last(R_1), \dots, Last(R_r))$.

The lattice is graded by the sum of distances from the triangles $First(R_i)$ of the minimal BCI tuple.

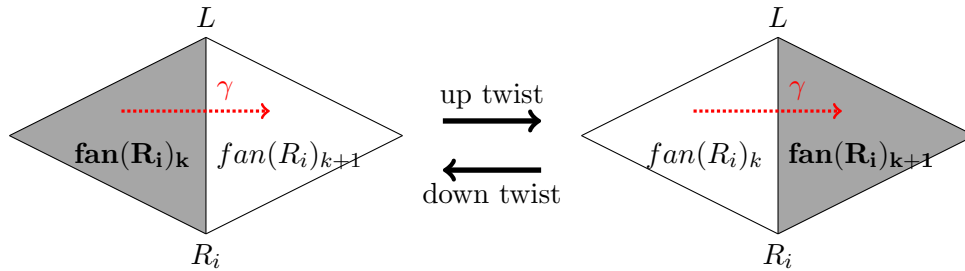


FIGURE 42. Twist of a BCI tuple.

Definition A.17 (twist). We define an up twist to be a local move that affects precisely one triangle $t_i = fan(R_i)_k$ of b , replacing $fan(R_i)_k$ with $fan(R_i)_{k+1}$. A down twist replaces $fan(R_i)_k$ with $fan(R_i)_{k-1}$. See Fig. 42.

Compare this twist of a triangle in a BCI tuple with [MSW13, Thm. 5.4], which explains how to do an up twist on a tile and (consequently, due to [MS10, Thm. 4.6]) a three-step subpath of the corresponding T -path. See Figure 43.

Even though we do not work with principal coefficients, it still makes sense to define a *height function* for each BCI tuple.

Definition A.18 (height function). Let

$$\tau_{R_i,1}, \tau_{R_i,2}, \dots, \tau_{R_i,f}$$

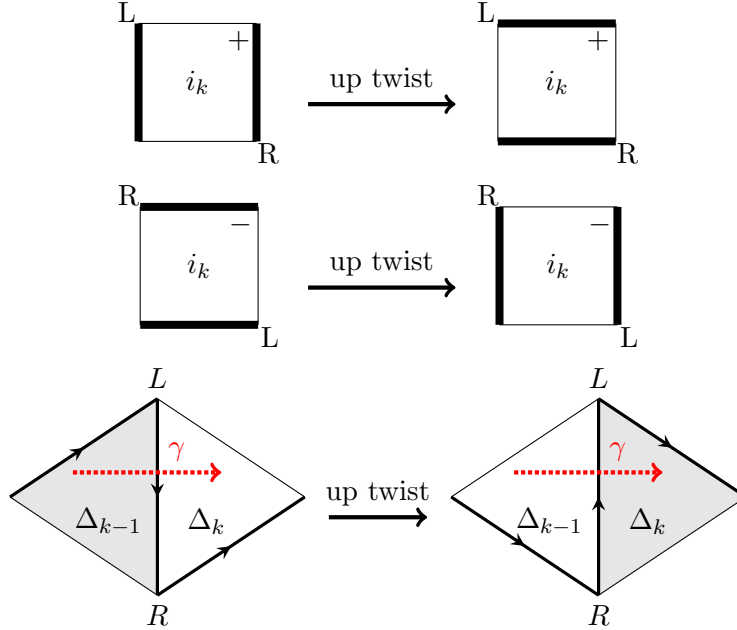


FIGURE 43. Two upper rows: An up twist on a snake graph tile. Bottom row: An up twist of a sequence of three steps of a T -path.

(where $f = |FAN(R_i)| - 1$) be the arcs crossed by γ and adjacent to R_i , ordered by the orientation of γ . Given an arbitrary BCI tuple $b = (t_1, \dots, t_r) = (\Delta(R_1), \dots, \Delta(R_r))$, we define its height function $h(b)$ by the monomial

$$\left(\prod_k w(\tau_{R_1,k}) \right) \left(\prod_k w(\tau_{R_2,k}) \right) \dots \left(\prod_k w(\tau_{R_r,k}) \right)$$

where each inner product is taken over every k such that $\tau_{R_i,k}$ is an edge between triangles $\Delta(R_i)$ and $First(R_i)$. By convention, if $\Delta(R_i) = First(R_i)$, there is no edge between them, and the product equals 1.

Proposition A.19 (Analog of [MSW13, Theorem 5.2]). *Construct a graph $L_{BCI}(\gamma)$ whose vertices are labeled by BCI tuples for γ , and whose edges connect two vertices if and only if the two tuples are related by an up or down twist. This graph is the Hasse diagram of a distributive lattice, whose minimal element is the minimal BCI tuple of γ . The lattice is graded by the degree of each height function.*

We describe how to read off from T and γ a poset Q_γ whose lattice of order ideals $J(Q_\gamma)$ is equal to $L_{BCI}(\gamma)$. The following definition is equivalent to [MSW13, Def. 5.3].

Definition A.20 (poset Q_γ). *We associate to \tilde{S}_γ and γ a directed graph Q_γ whose vertices are labeled by $1, \dots, d$, and whose directed edges are described as follows. Put an arrow from k to $k+1$ if and only if $\tau_{i_{k+1}}$ follows τ_{i_k} (considered as sides of Δ_k) in the counterclockwise order (see Fig. 44). Because \tilde{S}_γ is a triangulated polygon, the underlying undirected graph of Q_γ is a Dynkin diagram of type A . By abuse of notation, let Q_γ denote the poset whose Hasse diagram is Q_γ .*

Remark A.21. *As a corollary of [MSW13, Theorem 5.4], we have the following facts. The lattice $L_{BCI}(\gamma)$ from Proposition A.19 is isomorphic to the lattice of order ideals $J(Q_\gamma)$ of the poset Q_γ from Definition A.20; the support of the height monomial of a BCI tuple b consists precisely of*

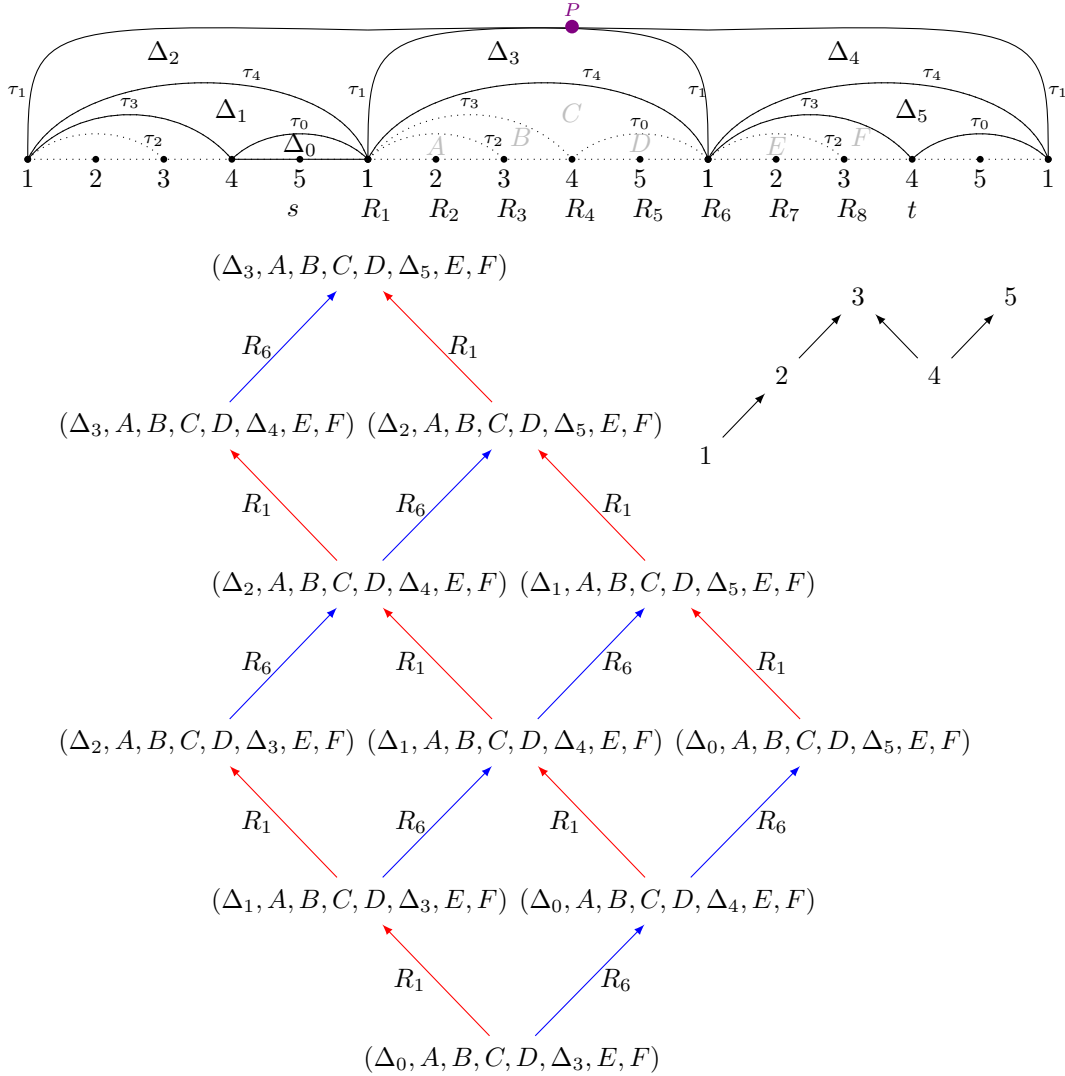


FIGURE 44. Based on the setup of Figure 30 (redrawn at the top). Left: the lattice $L_{BCI}(\gamma)$ of the BCI tuples for γ . Right: the poset Q_γ .

the elements in the corresponding order ideal. Moreover, an up twist of an entry of the tuple b corresponds to going up in the poset.

REFERENCES

[BCI74] D. Broline, D. W. Crowe, and I. M. Isaacs. The geometry of frieze patterns. *Geometriae Dedicata*, 3:171–176, 1974.

[BD14] Karin Baur and Grégoire Dupont. Compactifying exchange graphs I: Annuli and tubes. *Ann. Comb.*, 18(3):383–396, 2014.

[BFPT16] Karin Baur, Klemens Fellner, Mark James Parsons, and Manuela Tschabold. Growth behaviour of periodic tame friezes. *arXiv preprint arXiv:1603.02127*, 2016.

[BM09] Karin Baur and Robert J. Marsh. Frieze patterns for punctured discs. *J. Algebraic Combin.*, 30(3):349–379, 2009, 0711.1443.

[BPT16] Karin Baur, Mark J. Parsons, and Manuela Tschabold. Infinite friezes. *European J. Combin.*, 54:220–237, 2016.

[CC73] John H Conway and HSM Coxeter. Triangulated polygons and frieze patterns. *The Mathematical Gazette*, 57(400):87–94, 1973.

- [CC06] Philippe Caldero and Frédéric Chapoton. Cluster algebras as Hall algebras of quiver representations. *Comment. Math. Helv.*, 81(3):595–616, 2006.
- [CLS15] Ilke Canakci, Kyungyong Lee, and Ralf Schiffler. On cluster algebras from unpunctured surfaces with one marked point. *Proc. Amer. Math. Soc. Ser. B*, 2:35–49, 2015.
- [Cox71] H. S. M. Coxeter. Frieze patterns. *Acta Arith.*, 18:297–310, 1971.
- [CP03] Gabriel D. Carroll and Gregory Price. Two new combinatorial models for the ptolemy recurrence. *unpublished memo*, 2003.
- [CS13] Ilke Canakci and Ralf Schiffler. Snake graph calculus and cluster algebras from surfaces. *J. Algebra*, 382:240–281, 2013.
- [CS15a] Ilke Canakci and Ralf Schiffler. Snake graph calculus and cluster algebras from surfaces II: self-crossing snake graphs. *Math. Z.*, 281(1-2):55–102, 2015.
- [CS15b] Ilke Canakci and Ralf Schiffler. Snake graph calculus and cluster algebras from surfaces iii: Band graphs and snake rings. *arXiv preprint arXiv:1506.01742*, 2015.
- [Dev16] The Sage Developers. *SageMath, the Sage Mathematics Software System (Version 7.3)*, The Sage Development Team, 2016. <http://www.sagemath.org>.
- [DT13] Grégoire Dupont and Hugh Thomas. Atomic bases of cluster algebras of types A and \tilde{A} . *Proc. Lond. Math. Soc.*, 107(4):825–850, 2013, 1106.3758.
- [FST08] Sergey Fomin, Michael Shapiro, and Dylan Thurston. Cluster algebras and triangulated surfaces. I. Cluster complexes. *Acta Math.*, 201(1):83–146, 2008, math.RA/0608367.
- [FT12] Sergey Fomin and Dylan Thurston. Cluster algebras and triangulated surfaces. part II: Lambda lengths. *arXiv preprint arXiv:1210.5569*, 2012.
- [GM15] Emily Gunawan and Gregg Musiker. T -path formula and atomic bases for cluster algebras of type D . *SIGMA Symmetry Integrability Geom. Methods Appl.*, 11:060, 46 pages, 2015.
- [MS10] Gregg Musiker and Ralf Schiffler. Cluster expansion formulas and perfect matchings. *J. Algebraic Combin.*, 32(2):187–209, 2010, 0810.3638.
- [MSW11] Gregg Musiker, Ralf Schiffler, and Lauren Williams. Positivity for cluster algebras from surfaces. *Adv. Math.*, 227(6):2241–2308, 2011, 0906.0748.
- [MSW13] Gregg Musiker, Ralf Schiffler, and Lauren Williams. Bases for cluster algebras from surfaces. *Compos. Math.*, 149(2):217–263, 2013, 1110.4364.
- [Mul13] Greg Muller. Locally acyclic cluster algebras. *Adv. Math.*, 233:207–247, 2013.
- [MW13] Gregg Musiker and Lauren Williams. Matrix formulae and skein relations for cluster algebras from surfaces. *Int. Math. Res. Not. IMRN*, (13):2891–2944, 2013.
- [Pro02] James Propp. Lattice structure for orientations of graphs. *arXiv preprint math/0209005*, 2002.
- [Pro05] James Propp. The combinatorics of frieze patterns and markoff numbers. *arXiv preprint math/0511633*, 2005.
- [SCc08] The Sage-Combinat community. *Sage-Combinat: enhancing Sage as a toolbox for computer exploration in algebraic combinatorics*, 2008. <http://combinat.sagemath.org>.
- [Sch08a] Ralf Schiffler. A cluster expansion formula (A_n case). *Electron. J. Combin.*, 15(1):Research paper 64, 9, 2008.
- [Sch08b] Ralf Schiffler. A geometric model for cluster categories of type D_n . *J. Algebraic Combin.*, 27(1):1–21, 2008, math.RT/0608264.
- [Sch10] Ralf Schiffler. On cluster algebras arising from unpunctured surfaces. II. *Adv. Math.*, 223(6):1885–1923, 2010, 0809.2593.
- [Smi15] David Smith. Infinite friezes and triangulations of the strip. *arXiv preprint arXiv:1512.05842*, 2015.
- [ST09] Ralf Schiffler and Hugh Thomas. On cluster algebras arising from unpunctured surfaces. *Int. Math. Res. Not.*, 2009(17):3160–3189, 2009, 0712.4131.
- [SZ04] Paul Sherman and Andrei Zelevinsky. Positivity and canonical bases in rank 2 cluster algebras of finite and affine types. *Mosc. Math. J.*, 4(4):947–974, 2004, math.RT/0307082.
- [Thu14] Dylan Paul Thurston. Positive basis for surface skein algebras. *Proc. Natl. Acad. Sci. USA*, 111(27):9725–9732, 2014.
- [Tsc15] Manuela Tschabold. Arithmetic infinite friezes from punctured discs. *arXiv preprint arXiv:1503.04352*, 2015.
- [Yur16] Toshiya Yurikusa. A new cluster expansion formula for cluster algebras in type A . *arXiv preprint arXiv:1605.07557*, 2016.

GUSTAVUS ADOLPHUS COLLEGE, 800 WEST COLLEGE AVENUE, SAINT PETER, MN 56082, USA
E-mail address: `egunawan@math.umn.edu`

DEPARTMENT OF MATHEMATICS, UNIVERSITY OF MINNESOTA, MINNEAPOLIS, MN, USA
E-mail address: `musiker@math.umn.edu`

DEPARTMENT OF MATHEMATICS AND SCIENTIFIC COMPUTING, UNIVERSITY OF GRAZ, GRAZ, AUSTRIA
E-mail address: `hannah.vogel@uni-graz.at`